Title
Mesenchymal-endothelial transition contributes to cardiac neovascularization.

Journal
Nature, 514(7524)

ISSN
0028-0836

Authors
Ubil, Eric
Duan, Jinzhu
Pillai, Indulekha CL
et al.

Publication Date
2014-10-01

DOI
10.1038/nature13839

Peer reviewed

HHS Public Access

Author manuscript

Nature. Author manuscript; available in PMC 2015 April 30.

Published in final edited form as:

Nature. 2014 October 30; 514(7524): 585–590. doi:10.1038/nature13839.

Mesenchymal-endothelial-transition contributes to cardiac neovascularization

Eric Ubil[9,*], **Jinzhu Duan**[1,2,3,4,5,6,*], **Indulekha C.L. Pillai**[1,2,3,4,5,6], **Manuel Rosa-Garrido**[1,2,7,8], **Yong Wu**[2,7], **Francesca Bargiacchi**[10], **Yan Lu**[1,2,3,4,5,6], **Seta Stanbouly**[1,2,3,4,5,6], **Jie Huang**[1,2,3,4,5,6], **Mauricio Rojas**[11], **Thomas M. Vondriska**[1,2,6,7,8], **Enrico Stefani**[2,7,8], and **Arjun Deb**[1,2,3,4,5,6,**]

[1]Division of Cardiology, Department of Medicine, David Geffen School of Medicine & College of Letters and Sciences, University of California, Los Angeles

[2]Department of Molecular Cellular and Developmental Biology, David Geffen School of Medicine & College of Letters and Sciences, University of California, Los Angeles

[3]Cardiovascular Research Laboratory, David Geffen School of Medicine & College of Letters and Sciences, University of California, Los Angeles

[4]Eli and Edythe Broad Institute of Regenerative Medicine and Stem Cell Research, David Geffen School of Medicine & College of Letters and Sciences, University of California, Los Angeles

[5]Jonsson Comprehensive Cancer Center, David Geffen School of Medicine & College of Letters and Sciences, University of California, Los Angeles

[6]Molecular Biology Institute, David Geffen School of Medicine & College of Letters and Sciences, University of California, Los Angeles

[7]Division of Molecular Medicine, Department of Anesthesiology, David Geffen School of Medicine & College of Letters and Sciences, University of California, Los Angeles

[8]Department of Physiology, David Geffen School of Medicine & College of Letters and Sciences, University of California, Los Angeles

[9]Department of Cell Biology & Physiology, McAllister Heart Institute, University of North Carolina, Chapel Hill

Address correspondence to: Arjun Deb, 675 Charles E Young Drive S, MRL 3609, University of California, Los Angeles, Los Angeles, CA 90095, adeb@mednet.ucla.edu, Phone: (1) 919-672-1003 Fax: (1) 310-206-5777.

*Both authors contributed equally to this work

**This work was initiated when AD was at the University of North Carolina, Chapel Hill and completed at the University of California, Los Angeles

Author Contributions

E.U. and J.D. performed experiments, obtained and analyzed data and did statistical analysis. I.P., Y.W. and E.S. performed super-resolution microscopy experiments. I.P., S.S. and J.H. performed flow cytometry and *in vitro* experiments. M.R.G. and T.M.V. performed ChIP experiments. F.B. did Western blotting. M.R. and Y.L. performed animal surgeries and echocardiograms. A.D. conceptualized the project, performed statistical analysis, supervised the work and wrote the manuscript.

The authors have no competing financial interests to disclose.

Extended data figures are linked to the online version of the paper at www.nature.com/nature

[10]Department of Pharmacology, McAllister Heart Institute, University of North Carolina, Chapel Hill

[11]Department of Medicine, McAllister Heart Institute, University of North Carolina, Chapel Hill

Abstract

Endothelial cells contribute to a subset of cardiac fibroblasts by undergoing endothelial-to-mesenchymal-transition, but whether cardiac fibroblasts can adopt an endothelial cell fate and directly contribute to neovascularization after cardiac injury is not known. Here, using genetic fate map techniques, we demonstrate that cardiac fibroblasts rapidly adopt an endothelial cell like phenotype after acute ischemic cardiac injury. Fibroblast derived endothelial cells exhibit anatomical and functional characteristics of native endothelial cells. We show that the transcription factor p53 regulates such a switch in cardiac fibroblast fate. Loss of p53 in cardiac fibroblasts severely decreases the formation of fibroblast derived endothelial cells, reduces post infarct vascular density and worsens cardiac function. Conversely, stimulation of the p53 pathway in cardiac fibroblasts augments mesenchymal to endothelial transition, enhances vascularity and improves cardiac function. These observations demonstrate that mesenchymal-to-endothelial-transition contributes to neovascularization of the injured heart and represents a potential therapeutic target for enhancing cardiac repair.

The mammalian heart after acute injury heals primarily by fibrosis. Cardiac fibroblasts proliferate at the site of injury[1] and fibroblast proliferation is accompanied by recruitment of endothelial cells. Endothelial cells contribute to neovascularization of the injury region[2] and promote repair[3]. A close interaction between fibroblasts and endothelial cells is thought to regulate wound healing[4]. A subset of endothelial cells, by undergoing endothelial-mesenchymal-transition, generates fibroblasts in the injury region[5] and cardiac fibroblasts express pro-angiogenic molecules that in turn promote angiogenesis[6,7]. However cardiac fibroblasts are thought to be terminally differentiated cells[8,9] and whether they have the ability to adopt an endothelial phenotype and directly contribute to neovascularization after cardiac injury is not known. Here, we demonstrate that cardiac fibroblasts undergo mesenchymal-endothelial-transition (MEndoT) to generate *de novo* endothelial cells in the injured heart and show that MEndoT can be augmented to enhance cardiac repair.

Cardiac fibroblasts adopt an endothelial cell like fate after ischemic cardiac injury

We used a genetic fate map strategy to label cardiac fibroblasts, by crossing transgenic mice harboring a tamoxifen inducible Cre recombinase driven by fibroblast specific regulatory sequence of the alpha2 (type 1) collagen gene (Col1a2CreERT)[10–12] with the lineage reporter strain (Rosa26R^{tdTomato})[13] to create Col1a2CreERT:Rosa26R^{tdTomato} progeny mice. In these mice, administration of tamoxifen results in activation of Cre recombinase and cells expressing Col1a2 at the time of tamoxifen administration are irreversibly labeled by tdTomato fluorescence. We administered tamoxifen for 10 days to adult Col1a2CreERT:R26R^{tdTomato} mice. Five days following cessation of tamoxifen, we observed that approximately 55% of all non-myocyte cells exhibited tdTomato fluorescence

and greater than 96% and 99% of tdTomato fluorescent cells expressed the cardiac fibroblast markers Domain Discoidin Receptor 2 (DDR2) and vimentin (Extended Data Fig. 1a–c). Immunofluorescent staining showed that 87±9% and 99±0.5% (mean±S.E.M) of tdTomato labeled cells expressed DDR2 and vimentin respectively, supporting flow cytometry data (Extended Data Fig. 1d,e). tdTomato cells did not express endothelial markers VECAD and CD31 (99.9±0.06% and 99.8±0.02% negative respectively, mean±S.E.M.) (Extended Data Fig. 1f,g), did not express the cardiac progenitor marker C-Kit nor markers of smooth muscle, macrophages, and lymphatics (Extended Data Fig. 1h–k). Cardiac myocytes did not express Cre recombinase as previously shown[10]. Taken together these data strongly suggest that cells exhibiting tdTomato fluorescence in hearts of Col1a2CreERT:R26R^{tdTomato} mice are cardiac fibroblasts and do not express canonical markers of other cardiovascular cell types.

We subjected Col1a2CreERT:R26R^{tdTomato} mice to ischemia-reperfusion cardiac injury 5 days following cessation of tamoxifen injection. By day 3 post-injury, 35±3% (mean ±S.E.M) of labeled cardiac fibroblasts in the region of injury expressed the endothelial specific marker VECAD, while in sham injured animals only rare labeled cells expressed VECAD (<0.3%) (Fig. 1a–c). Approximately 24±4%, 44±4% and 35±3% (mean±S.E.M) of labeled cardiac fibroblasts also expressed other endothelial markers such as endothelial nitric oxide synthase (eNOS) and the endothelial tight junctional proteins Claudin 5[14] and Occludin[14] respectively (Fig. 1a–c). MEndoT was most pronounced in the injury border zone significantly decreasing in regions remote from the infarct. (Fig. 1c). The fraction of cardiac fibroblasts expressing VECAD increased between 1 and 3 days post-injury and remained similar at 3, 7 and 14 days (Fig. 1d). The fraction of tdTomato positive cells expressing VECAD in sham injured animals at 3, 7 and 14 days was 0.3±0.1%, 1.4±1.4% and 0.6±0.4% (mean±S.E.M., $p>0.05$, one way Anova) demonstrating no temporal difference in the fraction of tdTomato labeled cells expressing VECAD following sham injury.

As fibroblasts lie in close apposition to endothelial cells and pericytes, we performed super-resolution microscopy to validate our observations with confocal microscopy. Stimulated emission deletion (STED) microscopy is a form of super-resolution microscopy that provides an average lateral resolution of 30–40nm compared to confocal microscopy that provides an average lateral resolution of 250nm[15]. Using STED we observed that tdTomato cells after injury express VECAD and can be distinguished from closely apposed endothelial cells not expressing tdTomato label (Fig. 1e). STED microscopy also demonstrated that tdTomato cells did not express pericyte markers NG2 or CD146 (Extended Data Fig. 1l,m).

We next investigated whether fibroblast derived endothelial cells incorporate into capillaries in the infarct border zone. We perfused Col1a2CreERT:R26R^{tdTomato} mice with a fluorescent lipophilic dye DiO that labels endothelial cell membranes and has been used to identify the vasculature of solid organs including the heart[16]. In both longitudinal (Fig. 1f,g) and transverse sections of capillaries (Fig. 1h) in the injury border zone, we observed endothelial cells bearing the fibroblast label to line the lumen of the blood vessel but the contribution was minimal in sham injured animals (Fig 1f). Luminal DiO+ tdTomato+ cells expressed VECAD (Extended Data Fig. 2a) thus confirming the endothelial phenotype.

Luminal surface area occupied by fibroblast derived endothelial cells peaked at 7 days post-injury and remained similar at 14 days (Fig. 1i). Endothelial cells are known to take up acetylated LDL (AcLDL)[17]. We systemically injected Col1a2CreERT:R26R^{tdTomato} mice 3 days after cardiac injury with fluorescent labeled AcLDL and observed that, 41±8% (mean ±S.E.M) of fibroblast derived endothelial cells took up AcLDL demonstrating their functional similarity to native endothelial cells (Fig. 1j).

A subset of cardiac fibroblasts after cardiac injury become myofibroblasts and express α-smooth muscle actin (αSMA)[18,19]. We stained for αSMA and showed that 3 days after injury, 11±3% (mean±S.E.M.) of labeled cardiac fibroblasts in the injured region expressed αSMA but very few labeled cells co-expressed αSMA and VECAD, suggesting that cardiac fibroblasts undergoing MEndoT are distinct from myofibroblasts (Extended Data Fig. 2b–f).

We next determined whether substantial recombination in endothelial cells (i.e. leaky promoter elements) could potentially confound our findings. Stochastic induction of Cre can occur after cardiac injury[20]. We injected Col1a2CreERT:R26R^{tdTomato} animals with vehicle (corn oil) instead of tamoxifen and observed rare labeled cardiac fibroblasts (<0.07% at 3 and 7 days) after ischemic injury demonstrating that injury alone did not lead to significant Cre activation (Extended Data Fig. 3a–c).

Endothelial cells are known to undergo endothelial-mesenchymal-transition (EndMT) and adopt a fibroblast phenotype after cardiac injury[5]. We investigated whether endothelial cells undergoing EndMT would exhibit tdTomato fluorescence and be mistakenly included in our analysis. We performed immunofluorescent staining for Col1 and observed that approximately 6±1% (mean±S.E.M.) of endothelial cells after injury expressed Col1 but none of these cells exhibited tdTomato fluorescence (Extended Data Fig. 3d). Conversely tdTomato labeled cells in the injury region that expressed VECAD did not stain for Col1 (Extended Data Fig. 3e). Next, we crossed Col1a2CreERT:R26R^{tdTomato} mice with the Col1-GFP transgenic mice, which have GFP expression directly driven by the Col1a1 promoter. GFP expression thus serves as a useful real-time reporter of Col1 expression[21,22]. Progeny mice (Col1a2CreERT:R26R^{tdTomato}:Col1-GFP) were administered tamoxifen and subjected to ischemic myocardial injury. At 3 days post-injury, tdTomato labeled cells that expressed VECAD did not exhibit GFP fluorescence (Extended Data Fig. 4a). Approximately 3±1% (mean±S.E.M.) of VECAD positive cells were GFP positive but with the exception of rare cells, VECAD+GFP+ cells did not exhibit tdTomato fluorescence (**Extended** Fig. 4b).

Immunofluorescent staining for Cre protein in Col1a2CreERT:R26R^{tdTomato} mice hearts after injury demonstrated that tdTomato+VECAD+ cells did not express Cre (Extended Data Fig 4c–i) consistent with the earlier observation that that these cells do not express type 1 Collagen. In the absence of tamoxifen, tdTomato cells expressing Col1a2 would be expected to have Cre in their cytoplasm. In hearts of Col1a2CreERT:R26R^{tdTomato}:Col1-GFP mice tdTomato labeled cells that expressed type 1 collagen (GFP positive) exhibited cytoplasmic but not nuclear Cre staining. (Extended Data Fig. 4j–m). Taken together, these observations demonstrate the fidelity of the Cre driver and argue against a “leaky” Cre as the basis for our findings.

Next we investigated whether Col1a2 expressing endothelial progenitors in the heart or bone marrow could have been labeled during administration of tamoxifen and subsequently generated tdTomato+ endothelial cells. We analyzed the heart and bone marrow but observed less than 0.5% of tdTomato cells in the heart (Extended Data Fig. 5a,b) or bone marrow (Extended Data Fig. 5c–f) to express endothelial progenitor markers (CD133 CD34 and Flk1)[23]. Bone marrow derived mesenchymal stem cells did not exhibit tdTomato fluorescence with the exception of rare cells (Extended Data Fig. 5g). Collectively, these observations suggest that substantial labeling of endothelial progenitors did not occur making them an unlikely source of tdTomato+ endothelial cells.

Finally, we subjected FSP1Cre:R26R^{tdTomato} mice to ischemic cardiac injury to confirm MEndoT with another Cre driver. The FSP1Cre has been used to track cardiac fibroblast after *in vivo* reprogramming[8,9]. By day 3 post injury, 31±4% and 23±5% of tdTomato labeled cells in the injury region expressed the endothelial markers isolectin and VECAD compared to 2±1% and 4±1% in sham injured animals (Extended Data Fig. 6a–c) confirming MEndoT observations made using the Col1a2CreERT driver.

p53 mediates MEndoT *ex vivo*

We next investigated the mechanisms regulating MEndoT and hypothesized that cellular stress after cardiac injury plays a role in MEndoT. p53 is an important cellular stress response gene[24], modulates reprogramming[25] and regulates epithelial-mesenchymal-transition[26]. We observed that 37% of tdTomato labeled cardiac fibroblasts expressed p53 at 3 days post injury. In contrast, rare labeled cells expressed p53 in the sham injured heart (Fig. 2a,b). p53 expression in labeled fibroblasts peaked at 7 days after cardiac injury (Fig. 2c). By day 7 after injury, approximately 91±7% (mean±S.E.M.) of tdTomato labeled cells expressing p53 co-expressed VECAD (Fig. 2d), demonstrating a strong association between p53 and VECAD expression in tdTomato labeled cells.

To determine whether p53 plays a regulatory role in MEndoT, we first established an *ex vivo* model. Cells subjected to types of cellular stress *ex vivo*, such as serum deprivation, upregulate p53 levels[27,28]. We subjected cardiac fibroblasts to serum starvation and observed increased p53 levels by Western Blotting (Extended Data Fig. 7a,b). We next seeded labeled cardiac fibroblasts (99% purity by flow cytometry), on matrigel (a mixture of basement membrane proteins that facilitates capillary tube formation) and subjected them to serum starvation. In contrast to control fibroblasts (Fig. 2e,g) serum starved fibroblasts formed capillary tube like structures, expressed VECAD (Fig. 2f) and took up AcLDL (Fig. 2h), consistent with adoption of an endothelial cell like phenotype.

Using gain and loss of function approaches, we determined whether p53 affects serum starvation induced MEndoT (Fig. 2i–o). Serum deprivation induced cardiac fibroblasts to form tubes on matrigel (Fig. 2i,j) but addition of Pifithrin-α, an inhibitor of p53[29] decreased tube formation by 67% (Fig. 2k,n). Pifithrin-α did not have an effect on serum fed cardiac fibroblasts (Extended Data Fig. 7c,d). Next, we generated mice specifically deficient in fibroblast p53 by crossing Col1a2CreERT:R26R^{tdTomato} mice with mice having both p53 alleles floxed[30]. Progeny mice (Col1a2CreERT:R26R^{tdTomato}:p53$^{fl/fl}$), 8 weeks old, were

injected with tamoxifen to delete p53 and label Col1a2 expressing p53 deficient cells (tdTomato+). Cardiac fibroblasts were subsequently harvested and subjected to serum starvation. The absence of p53 decreased capillary tube formation on matrigel by 95% (Fig. 2l,n). We subsequently investigated whether activation of p53 signaling enhanced serum deprivation induced MEndoT. Cardiac fibroblasts subjected to serum starvation were treated with the small molecule RITA (**R**eactivation of p53 and **I**nduction of **T**umor **A**poptosis) that inhibits ubiquitin mediated p53 degradation and enhances p53 signaling[31]. RITA enhanced tube formation by 50% (Fig. 2m,n). RITA also increased tube formation in serum fed cardiac fibroblasts but to a lesser degree (Extended Data Fig. 7c,d). Following serum deprivation, qPCR demonstrated 4–20 fold increased expression of endothelial specific genes but treatment with Pifithrin-α or the genetic deletion of p53 in cardiac fibroblasts significantly blunted induction of endothelial gene expression (Fig. 2o). Conversely, treatment of serum starved cardiac fibroblasts with RITA significantly increased expression of endothelial specific genes by 3–7 fold (Fig. 2o). Interestingly, over-expressing p53 in wild type cardiac fibroblasts grown under serum fed conditions did not induce expression of VECAD or other endothelial specific genes suggesting that enhancing p53 signaling in the absence of serum starvation is not sufficient to induce MEndoT.

We next performed chromatin immunoprecipitation (ChIP) for p53 on serum starved cardiac fibroblasts and observed that p53 directly binds to promoter regions of endothelial specific genes and the endothelial transcription factors HoxA9[32] and HoxD3[33] that are known to play an important role for endothelial differentiation (Fig. 2p). Gene expression of HoxA9 and HoxD3 was also increased in cardiac fibroblasts by 6.53±1.74 and 7.18±1.16 fold respectively after serum starvation (mean±S.E.M., $p<0.05$ compared to cardiac fibroblasts in 10% serum). Although an indirect effect of p53 cannot be excluded, these observations suggest that p53 at least in this model initiates an endothelial gene expression program by directly inducing transcription of endothelial specific genes.

Using this *ex vivo* model, we next asked whether MEndoT was reversible. Transforming growth factor β(TGFβ) enhances EndMT[5] and TGFβ added to cardiac fibroblasts at the onset of serum starvation prevented tube formation (Extended Data Fig. 8a,b) and induction of VECAD expression (0.98±0.03 fold change in VECAD with TGFβ, mean± S.E.M. $p>0.05$, $n=3$). Moreover, when TGFβ was added to serum starved cardiac fibroblasts after they had already formed tubes, it led to 99% regression of tube formation (Extended Data Fig. 8c,d,g). A similar effect was observed with adding back serum (**Extended Fig. 8e,f,g**). VECAD expression also decreased by 56.4±2.4% (mean±S.E.M. $p<0.05$, $n=3$). Addition of Pifithrin-α to serum starved cardiac fibroblasts that had already formed tubes demonstrated significant disruption of formed tubes compared to PBS treated controls (**Extended Fig. 8h–n**). These observations suggest that p53 is required for maintaining the endothelial phenotype of the fibroblast derived endothelial like cell. Notably, the fraction of fibroblast derived endothelial cells was maintained at 14 days after cardiac injury *in vivo* (Fig. 1d, Fig. 2c) despite declining p53 levels suggestive of other factors stabilizing the endothelial phenotype.

p53 mediates MEndoT in the injured heart

To determine whether p53 mediates MEndoT *in vivo*, we subjected Col1a2CreERT:R26R^{tdTomato}:p53$^{fl/fl}$ mice to ischemic cardiac injury 5 days following cessation of tamoxifen. Mice with intact p53 exhibited 6±0.64 fold increase (mean±S.E.M.) in cardiac fibroblast p53 levels 3 days after cardiac injury, but in mice with fibroblast specific p53 deletion [referred to as Col1a2CreERT:R26R^{tdTomato}:p53CKO (conditional knock out)], the mean p53 expression in border zone cardiac fibroblasts failed to increase significantly (Fig. 3a–c). The degree of MEndoT at 3 days post-injury in Col1a2CreERT:R26R^{tdTomato}:p53CKO animals decreased by 57% (Fig. 3d–f) and was associated with a decrease in capillary density in the injury region (Fig. 3g). Increase in vessel density in the injured heart is a critical post-ischemic repair mechanism. Diminished neovascularization can lead to rapid decline in cardiac function after cardiac injury and is associated with worsened scarring[34]. Echocardiography on hearts of mice 7 days after cardiac injury showed significant worsening of cardiac function in p53CKO mice (Fig. 3h,i). Masson Trichrome staining demonstrated a greater amount of collagen deposition in the hearts of Col1a2CreERT:R26R^{tdTomato}:p53CKO animals (Fig. 3j,k). The degree of inflammatory infiltrate measured by the number of CD68 expressing macrophages was also significantly higher in the Col1a2CreERT:R26R^{tdTomato}:p53CKO animals (Extended Data Fig. 9a,b,d). These observations demonstrate that p53 is necessary for MEndoT to occur after ischemic cardiac injury and that disruption of MEndoT is associated with diminished post-injury vascularity and cardiac function.

We next looked at mechanisms inducing p53 expression in cardiac fibroblasts. C-terminal phosphorylation of Histone H2A family member X (γH2AX) is a DNA damage response pathway upstream of p53, is activated by hypoxic endothelial cells and shown to play a critical role in endothelial cell proliferation and hypoxic neovascularization[35]. We observed that 90% of tdTomato cells that up-regulated p53 co-expressed γH2AX suggesting that the γH2AX pathway is strongly associated with p53 expression in fibroblasts undergoing MEndoT (Extended Data Fig. 10a–c).

Stimulation of p53 pathway enhances MEndoT after acute ischemic cardiac injury

We investigated whether stimulation of p53 signaling after cardiac injury enhances MEndoT after acute ischemic cardiac injury. Col1a2CreERT:R26R^{tdTomato} animals injected with RITA daily for 3 days after cardiac injury exhibited significantly increased p53 expression in labeled fibroblasts (13±0.8 fold in RITA injected animals versus 6 fold increase in PBS injected animals) (Fig. 4a–c). RITA significantly enhanced the degree of MEndoT (Fig. 4d–f) and enhanced MEndoT was associated with a 26% increase in endothelial cells in the injury border zone (Fig. 4g). Increased neovascularization can lead to decreased collagen deposition and rapid improvement in post-injury cardiac function[3]. The area of collagen deposition 7 days after cardiac injury, decreased by 57% in RITA injected animals (Fig. 4h,i). Echocardiography demonstrated significantly improved cardiac function in RITA injected animals compared to PBS injected control animals (Fig. 4j,k).

Consistent with greater vascularity and better cardiac function, the inflammatory infiltrate was substantially reduced in RITA injected animals (**Extended Fig. 9a,c,d**). As RITA increases p53, we also looked at deleterious effects of increased p53 such as apoptosis. We subjected Col1a2CreERT:R26R^{tdTomato} animals to cardiac injury and consistent with published reports, did not observe increased p53 expression in myocytes after injury (Extended Data Fig. 9e,f) [36]. In RITA treated animals 3 days after injury there was not a significant increase in p53 expressing TUNEL stained nuclei compared to PBS injected controls (Extended Data Fig. 9g).

To demonstrate that increased MEndoT after administration of RITA was p53 dependent in cardiac fibroblasts, we injected RITA to Col1a2CreERT:R26R^{tdTomato}:p53CKO mice and observed that RITA failed to significantly enhance MEndoT. The degree of MEndoT was not statistically different from that observed in PBS treated Col1a2CreERT:R26R^{tdTomato}:p53CKO mice (Extended Data Fig. 9h,i). These observations suggest that RITA predominantly enhances MEndoT by activating p53 in cardiac fibroblasts.

Discussion

Our report suggests that cardiac fibroblasts possess a degree of native cellular plasticity that enables them to adopt endothelial cell like fates after cardiac injury. Recruitment and proliferation of endothelial cells in the ischemic heart is a critical cardiac repair response. Our data points to the fibroblast as a novel and robust source of endothelial cell generation in the injured heart. Mesenchymal-endothelial-transition, a hitherto unreported biological phenomenon appears to play an important physiological role in cardiac repair, as disruption of MEndoT worsened post-infarct vascularity and cardiac function. Teleologically, MEndoT provides the heart an efficient strategy to rapidly increase neovascularization in the injured region. The use of a small molecule to augment MEndoT and increase neovascularization after injury suggests that MEndoT may represent a therapeutic target for enhancing vascularity and repair of ischemic tissues.

METHODS

Animal care and use

All animal studies were approved by the Institutional Animal Care and Use Committee at the University of North Carolina, Chapel Hill and the University of California, Los Angeles.

Generation of transgenic and conditional knockout mice

Collagen1a2-CreERT:R26R^{tdTomato} mouse lines were obtained by crossing Collagen1a2-CreERT mice with lineage reporter R26R^{tdTomato} mice. To obtain Collagen1a2-CreERT:R26R^{tdTomato}:p53 CKO mice, Collagen1a2-CreERT:R26R^{tdTomato} mice were crossed to p53$^{fl/fl}$ mice and backcrossed to generate Collagen1a2-CreERT:R26R^{tdTomato}:p53$^{fl/fl}$ mice. Col1a2CreERT:R26R^{tdTomato} mice were crossed with Col1GFP mice to create progeny Col1a2CreERT:R26R^{tdTomato} :Col1GFP mice. FSP1Cre mice were crossed with the R26R^{tdTomato} mice to create FSP1Cre:R26R^{tdTomato} mice. Tamoxifen (1mg) (Sigma) was injected intra-peritoneally for 10 days to induce Cre-

mediated recombination in Col1a2CreERT mice. 5 days following cessation of tamoxifen animals were subjected to ischemic cardiac injury. All mice were on a C57B/6 background.

Murine cardiac injury model

All animal protocols were approved by the Institutional Animal Care and Use Committees at the University of North Carolina, Chapel Hill and at the University of California, Los Angeles. Animals (both male and female), 8–10 weeks old, were randomly allocated to sham or ischemia-reperfusion cardiac injury. Investigators performing surgeries and cardiac function studies were blinded to mouse genotype or treatment. Mice were initially anesthetized with 3% isoflurane, maintained at 2% isoflurane, and intubated using a Harvard Rodent Volume-Cycled Ventilator. Myocardial injury was induced by 30 minute ligation of the left anterior descending (LAD) coronary artery followed by reperfusion. Sham injury was performed in the same manner, with a ligature passed under the LAD, but the LAD was not ligated. No animals were excluded from analysis unless the animals died during the surgical procedure. At 1, 2, 3, 7, or 14 days after injury, the mice were anesthetized with pentobarbital (45mg/kg) and the left ventricle was perfused with 5ml PBS followed by 2ml 4% PFA. For RITA treated mice, RITA (Millipore) was administered intraperitoneally at 0.3mg/kg once daily for 3 days beginning 24 hours after injury. For AcLDL staining, 1μg fluorescent labeled AcLDL (Invitrogen) per gram body weight was injected via a catheter inserted in the jugular vein and hearts harvested as described 4 hours later. For DiO staining, DiO was prepared as described[16] and 2ml of 120μg/ml DiO perfused prior to PFA perfusion[16].

After perfusion, the heart was further fixed for 1 hour in 4% PFA at 4°C and after 1 hour the PFA was replaced with fresh 4% PFA and incubated at 4°C for another 3 hours. At the end of 4 hours, the hearts were sucrose embedded overnight in a 30% sucrose solution (MP Biochemicals) and then frozen in OCT (Tissue-Tek). 7μm sections were prepared in a longitudinal or transverse orientation. Group size was estimated based on previously observed mortality rates following surgery.

Echocardiography

Echocardiography was performed in conscious mice. The hair over the anterior chest was removed by a depilation cream and warmed Aquasonic gel applied over the thorax. Mice were held firmly by hand for the duration of the procedure (approximately 5 to 10 minutes) and conditioned daily for the procedure starting 3 days prior to the procedure. The probe was positioned over the chest in a parasternal position. Parasternal long axis B-mode and M-mode images are recorded. Measurements and analysis were then performed as described[10]. The echocardiographer was blinded to the genotype and treatment of the animal being examined.

Immunohistochemistry and histology, confocal imaging and quantitation, super-resolution microscopy

Immunofluorescent staining on frozen sections (7μm) was performed using primary antibodies to VECAD (Catalog#ab33168, Abcam), eNOS (Catalog#ab66127, Abcam), Claudin 5(Catalog#ab53765, Abcam), Occludin (Catalog#ab31721, Abcam), gamma

H2AX(Catalog#ab2893, Abcam), p53 (Catalog#ab31333 & ab26, Abcam), Col1 (Catalog#ab6308, Abcam), Podoplanin(Catalog#ab11936, Abcam), alpha-SMA (Catalog#ab5694, Abcam), CD68(Catalog#ab125212, Abcam), CD146 (Catalog#ab75769, Abcam), Cre (Catalog#BIOT-106L & PRB-106P,Covance), Troponin(Catalog#SC-8121, Santa Cruz), NG2 (Catalog# AB5320, EMD Millipore) and associated APC or Fluorescein conjugated secondary antibodies (Abcam, Millipore, Invitrogen) as per manufacturer instructions. Labeled sections were imaged using a Leica SP2 AOBS Upright Laser Scanning Confocal Microscope (Leica Microsystems). 5 independent images for each area (i.e. injury border zone, remote from injury, sham) were obtained and used for quantitative analysis. Colocalization analysis of confocal images was performed using Image J software (NIH). MEndoT percentages were derived by counting the number of dually labeled cells and dividing by the number of tdTomato positive cells. Quantitation of vascular area derived from fibroblasts was performed using the JACoP Image J plugin[37]. p53 expression levels in tdTomato positive cells were determined using the JACoP Image J plugin and expressed as a Manders coefficient normalized to p53 levels in sham injury[38]. In each case, 5 independent images from each area were analyzed from sections prepared from each mouse. For super-resolution microscopy, a custom made Stimulation Emission Depletion Super-resolution microscope was used. This microscope has a confocal channel for tdTomato and an ATTO647 flurophore super-resolution channel that was used for VECAD, NG2 or CD146 visualization. Masson-Trichrome staining was performed on heart sections as described[10].

Fibroblast isolation and culture

Cardiac fibroblasts were isolated from the explanted hearts of euthanized uninjured mice. The hearts were explanted and washed 3 times with 1X HBSS (Gibco). The heart was minced into approximately $1mm^2$ sized pieces and digested using 10ml of a 0.1% Trypsin solution (Gibco) with 50U/ml Collagenase II (Worthington)[39]. 5 sequential digestions were performed at 37°C, the cells collected and passed through a 40μM strainer and plated in IMDM, 1X Penicillin/Streptomycin, 10% FBS for 1 hour at 37°C. After 1 hour the medium was changed to F12K 1X Penicillin/Streptomycin, 10% FBS (Gibco), 10ng/ml leukemia inhibitory factor (LIF) (Millipore) and 10ng/ml basic Fibroblast growth factor (bFGF) (Millipore). Cells were maintained under these conditions until they became confluent in 7–10 days.

Matrigel tube formation and LDL uptake assay

6×10^4 fibroblasts per cm^2 were cultured overnight at 37°C, 5% CO_2 on Growth Factor Reduced Matrigel Basement Membrane Matrix (BD) coated wells of Nunc Lab-Tek II CC2 chamber slides (Thermo). Serum starved or unstarved cells were cultured in IMDM, 1X Penicillin/Streptomycin or IMDM, 1X Penicillin/Streptomycin, 10% fetal bovine serum (Gibco), respectively. Pifithrin-α 100μM (P4359, Sigma) or RITA 0.1μM (506149, EMD Chemicals) were added to the cells cultured with the above culture medium. Acetylated LDL (Invitrogen) uptake was performed as described[40].

Flow cytometry

Flow cytometric analysis for cell surface markers, were done using antibodies CD31-APC (Catalog#17-0311, eBioScience), CD34-FITC (Catalog#11-0341, eBiosience), CD133-FITC

(Catalog#11-1331, eBioscience), Flk1-APC (Catalog#17-5821, eBioscience), VECAD-APC (Catalog#17-1441, eBioscience), CD45-APC(Catalog#103111, Biolegend), ckit APC (Catalog#561074,BD Bioscience), DDR2 (Catalog#SC-7555,Santa Cruz) and Vimentin (Catalog#Ab1620, Millipore). For Vimentin and DDR2, a secondary APC conjugated anti-goat antibody was used (Catalog#SC3860, Santa Cruz). Cultured cardiac fibroblasts were dissociated using accutase (Innovative Cell Technologies, Inc.,) and immunostained in FACS buffer (0.1% BSA PBS) at 1×10^6/ml for 20–30 minutes at 4°C, followed by washing twice with FACS buffer and subsequently analyzed in Beckman-Coulter (Dako) CyAn ADP. Data obtained was analyzed and represented using Flowjo software.

Quantitative RT-PCR

RNA was isolated from cardiac fibroblasts cultured in the presence or absence of serum (IMDM, 1X Penicillin/Streptomycin, +/− 10% FBS), or in medium without serum and containing either 100μM Pifithrin-α or 0.1μM RITA, grown for 48 hours at 37°C, 5% CO_2. RNA isolation and reverse transcription was performed using the SV Total RNA Isolation Kit and the Reverse Transcription System (Promega). qPCR was performed using the SensiMix SYBR and Fluorescein Kit (Quantace) on an iQ5 thermal cycler (BioRad).

Western blot

Protein was harvested from cardiac fibroblasts cultured in the presence or absence of serum (IMDM, 1X Penicillin/Streptomycin, +/− 10% FBS) for 48 hours at 37°C, 5% CO_2. Concentration normalized protein was prepared with SDS loading buffer and run on a 12X Mini-Protean TGX gel (BioRad) at 300V for 25 min. The protein was transferred from the gel to a nitrocellulose membrane using the Trans-Blot Turbo System (BioRad). After blocking with TBST+3% cold fish gelatin, the membrane was probed using primary antibodies to p53 (Catalog#ab31333, Abcam) and alpha Tubulin (Catalog#T6199, Sigma), washed with TBST, and labeled using fluorescently conjugated secondary antibodies (LI-COR Biosciences). After washing with TBST, the membrane was visualized on an Odyssey scanner (LI-COR Biosciences). Densitometry analysis was performed using the Gel Analyzer unit of ImageJ software (NIH).

Chromatin Immunoprecipitation (ChIP)

Cardiac fibroblasts (30×10^6) were fixed in 1% formaldehyde, lysed in lysis buffer (50 mM Tris-HCl pH 8, 10 mM EDTA, 1% SDS, protease inhibitor cocktail Set I CALBIOCHEM) and sonicated using a EpiShear™ Multi-Sample Sonicator (Active Motif), leading to fragments between 300 and 1000 bp. ChIP was performed using a commercially available ChIP-IT High Sensitivity Kit (Active Motif) according to manufacturer's instructions. DNA-bound protein was immunoprecipitated using an anti-p53 antibody (Catalog#ab31333, Abcam) and anti IgG (Catalog#SC-2025, Santa Cruz) as a negative control. The DNA recovered was analyzed by quantitative real time-PCR using different primers sets that amplified the promoter region of Hoxa9, Hoxd3, CLDNS, Nos3 and negative control genes:

HoxA9 (1): (5′-TAAACTGCTCAGGCCATGCT -3′) sense / (5′-CAGCCTGGACCCACTGAAAG -3′) antisense

HoxD3 (1): (5′-TGCCTCAGTGTATTTCTCCCC -3′) sense / (5′-ATGGATAACAGTGCCCGGTG -3′) antisense

Claudin 5: (5′-CTCCGGAAGCCAACTTGGAG -3′) sense / (5′-GGACCCAGTGTGTCTAACCC -3′) antisense

eNOS: (5′-GGGACAGCCAGAAAATGGGA -3′) sense / (5′-ACTGCTGTCGGTCTCTTTGT -3′) antisense

Primers for p53 binding were designed using the SABiosciences' proprietary database (DECODE, DECipherment Of DNA Elements). Available from: http://www.sabiosciences.com/chipqpcrsearch PCR was performed with equal amounts of specific antibody immunoprecipitated sample, control (IgG) and Input. Values were normalized to input measurements and enrichment was calculated using the comparative Delta-DeltaCt (ΔΔCt) method. Data shown correspond to one representative assay (i.e. 3 PCRs) from a total of 3 independent assays each run with different sets of treated cells.

Statistical analysis

Statistical analysis was performed using GraphPad software (Prizm) using Student's t-test (2 tailed), one-way or two-way ANOVA with Bonferroni post test-analysis as appropriate. Welch's correction was used if variances between groups were significantly different. A p-value of < 0.05 was considered statistically significant. Graphs present the mean value ± standard error of the mean (SEM).

Extended Data

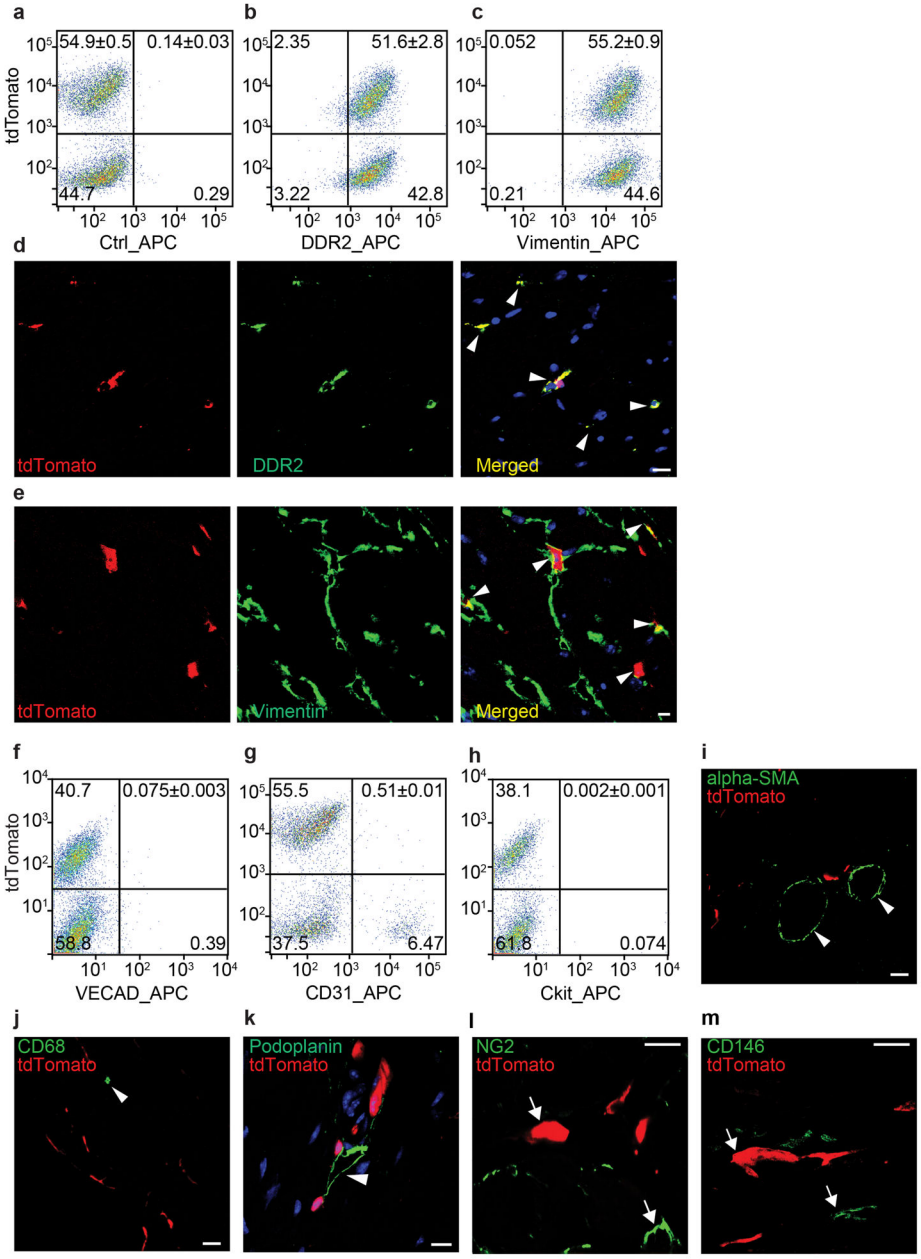

Extended Figure 1. Phenotypic characterization of tdTomato labeled cells in hearts of Col1a2CreERT:R26R^{tdTomato} mice

(a–c) Hearts were digested to obtain a non-myocyte population and subjected to flow cytometry to determine expression of **(b)** DDR2 and **(c)** vimentin. (**a**) serves as a control with no primary antibody added (number in each quadrant represents fraction of total population of cells). **(d,e)** Immunofluorescent staining on sham injured hearts of Col1a2CreERT:R26R^{tdTomato} mice to determine expression of **(d)** DDR2 (green) and **(e)** Vimentin (green) in tdTomato labeled cells (red) with merged image (right, arrowheads point to tdTomato labeled cells staining for DDR2 or vimentin. Scale bar: 10μm. **(f–h)** Non-

myocyte cells from the heart were subjected to flow cytometry to determine expression of **(f)** VECAD **(g)** CD31 or **(h)** c-Kit (number in each quadrant represents fraction of total population of cells) **(i–k)** Immunofluorescent staining for **(i)** alpha-smooth muscle actin **(j)** CD68 or **(k)** podoplanin was performed on frozen heart sections prepared from 8 week old sham injured Col1a2CreERT:R26R^{tdTomato} mice following tamoxifen injections and colocalization analysis performed to determine the number of labeled cardiac fibroblasts expressing alpha-smooth muscle actin (99.4% negative for alpha-SMA, 1500 cells examined), CD68 (100% negative for CD68, 1000 cells examined) or podoplanin (arrowheads). Scale bar: i–k: 10μm. (**l,m**) STED super-resolution microscopy demonstrating tdTomato labeled cells (arrows) not expressing **(l)** NG2 (green, arrows, STED channel) or **(m)** CD146 (green, arrows, STED channel). Scale bar: 10μm.

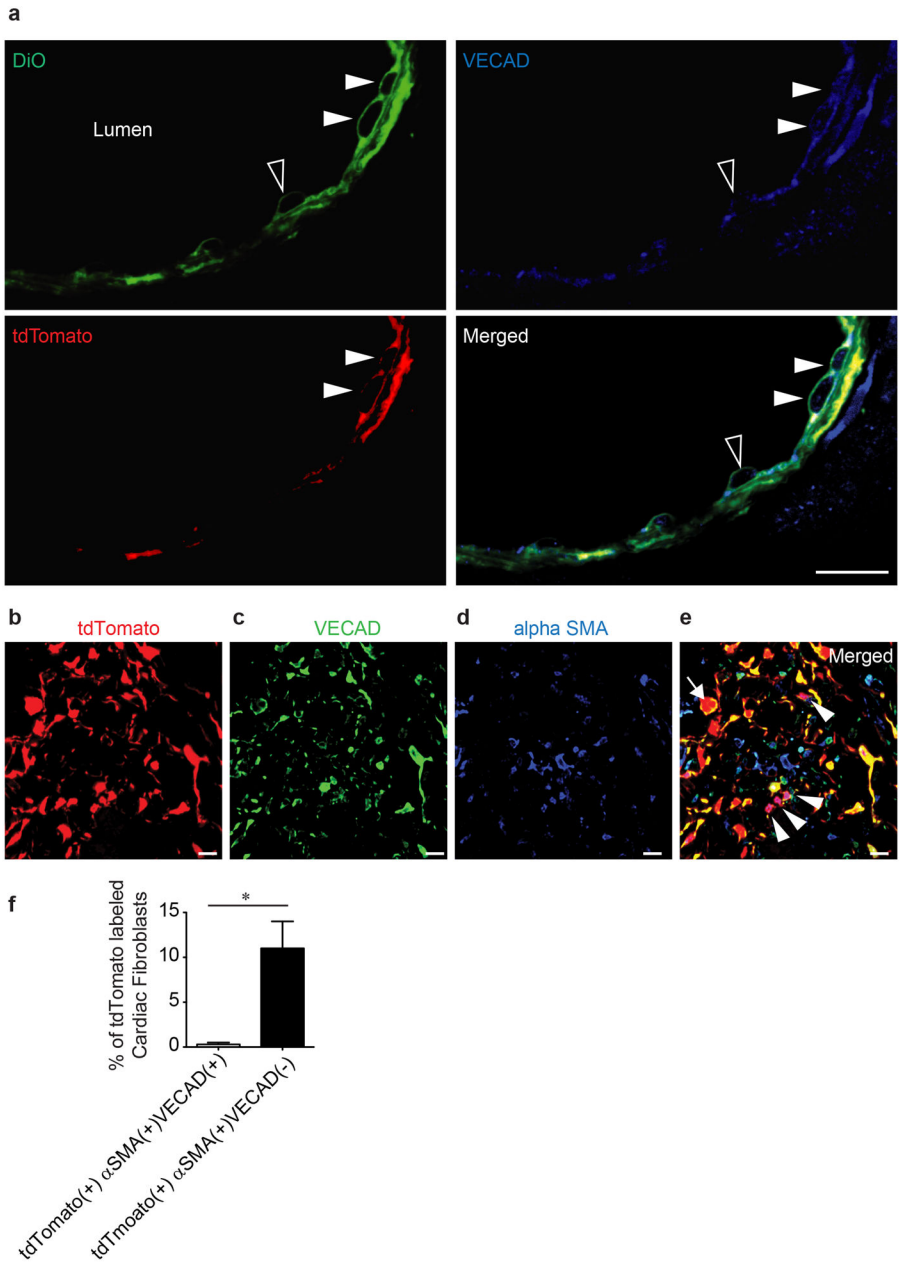

Extended Figure 2. Expression of VECAD in fibroblast derived endothelial cells that take up DiO and expression of alpha-smooth muscle actin and VECAD in tdTomato labeled cells

(a) Col1a2CreERT:R26R^{tdTomato} mice were subjected to ischemic injury, injected with DiO 7 days after cardiac injury and then harvested. High magnification of a wall of a blood vessel in the injured region demonstrates luminal cells staining for DiO (green, arrowheads), VECAD (blue, arrowheads), tdTomato (red, arrowheads) and merged image demonstrating colocalization of all three fluorophores (filled arrowheads); unfilled arrowhead points to VECAD+DiO+ cell that does not bear the tdTomato label. Scale bar: 10μm.

(b–f) Expression of alpha-smooth muscle actin and VECAD in tdTomato labeled cells

(b–e) Tamoxifen injected Col1a2CreERT:R26R^{tdTomato} mice underwent ischemia reperfusion injury and hearts were harvested 3 days after injury and immunofluorescent

staining performed for alpha-smooth muscle actin and VECAD. Section shows **(b)** tdTomato labeled cardiac fibroblasts **(c)** VECAD **(d)** alpha smooth muscle actin expressing cells and **(e)** merged image showing colocalization of fluorophores. Arrowheads show labeled cardiac fibroblasts expressing alpha smooth muscle actin and arrow shows a labeled cardiac fibroblast expressing VECAD but not smooth muscle actin. Scale bar: b–e: 10μm **(f)** Fraction of labeled cardiac fibroblasts that are alpha-smooth muscle actin+ and VECAD+ or VECAD- (mean±S.E.M., *p<0.05, n=3).

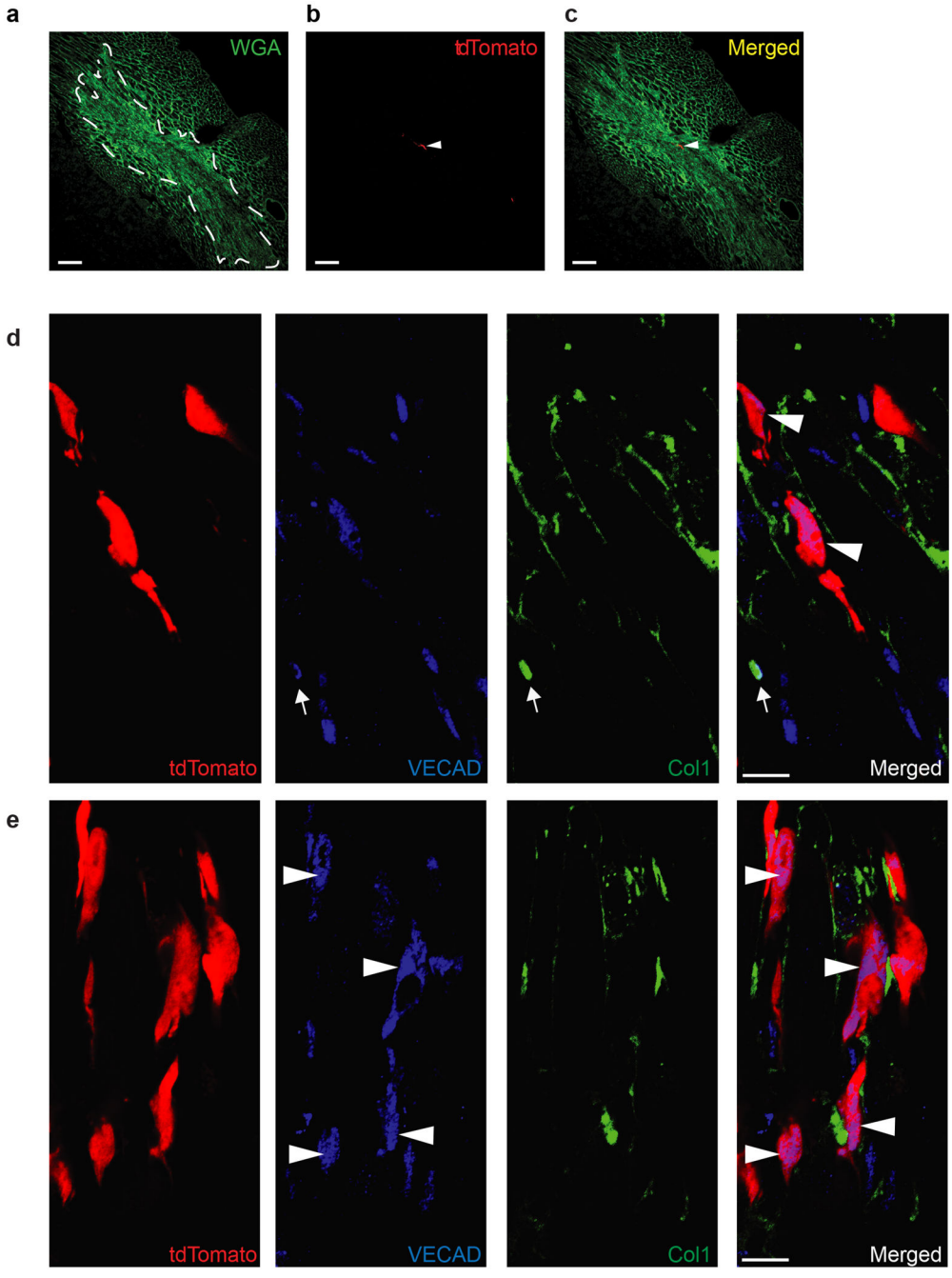

Extended Figure 3. tdTomato expression in hearts of vehicle injected Col1a2CreERT:R26R^{tdTomato} mice and immunostaining for Col1 and VECAD in tamoxifen injected Col1a2CreERT:R26R^{tdTomato} mice after cardiac injury

(a–c) Oil injected Col1a2CreERT:R26R^{tdTomato} mice underwent ischemia reperfusion injury and 3 days after injury, hearts were harvested and sectioned. Area of injury (demarcated by white lines) was stained with **(a)** Alexa488 labeled wheat germ agglutinin (WGA, stains cell membranes) **(b)** rare tdTomato expressing cells in same field (arrowhead) and **(c)** merged image showing the presence of rare labeled cells in the injury region (arrowhead) (28 labeled cells out of 38,000 cells counted (0.07%), n=3 animals). Scale bar: 100 μm. **(d,e)** Col1a2Cre:R26R^{tdTomato} (injected with tamoxifen as described in text) were subjected to ischemic cardiac injury and hearts harvested 3 days post injury and stained for Col1 and VECAD **(d)** Region of injury demonstrating a VECAD expressing cell (blue, arrow) staining positive for Col1 (green) but negative for the tdTomato label (merged arrow). Arrowheads in merged panel show tdTomato labeled cells expressing VECAD but not Col1. Scale bar: 10μm **(e)** tdTomato labeled cells expressing VECAD (arrowheads) that do not stain for Col1 (green) with merged image showing tdTomato+VECAD+ cells not staining with the Col1 antibody. Out of 225 cells counted (n=3 animals), we did not observe a single tdTomato+VECAD+ cell to stain for Col1. Conversely, not a single VECAD+Col1+ cell exhibited tdTomato fluorescence. Scale bar: 10μm.

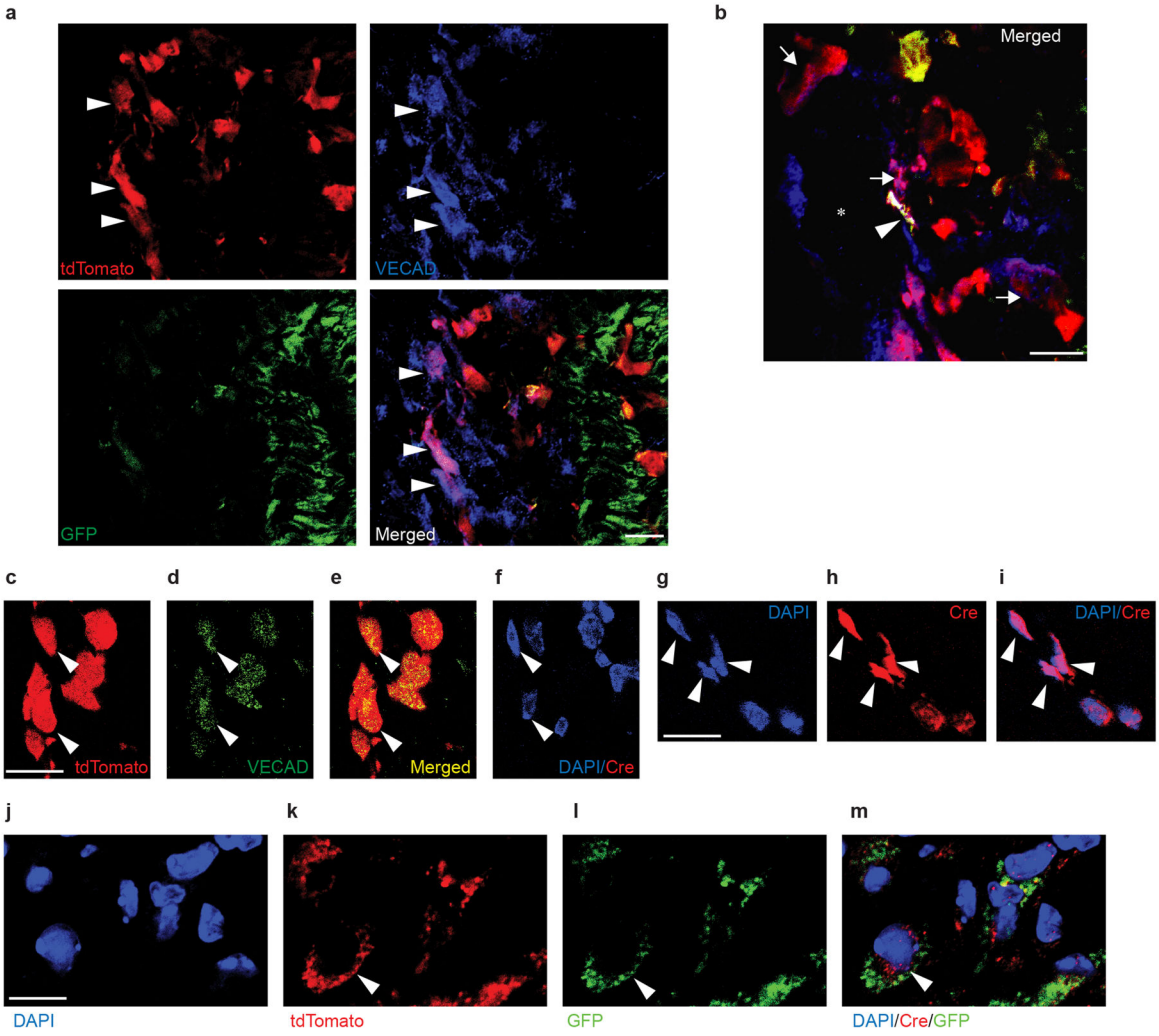

Extended Figure 4. VECAD and Cre immunostaining in heart sections of Col1a2Cre:R26R^{tdTomato}:Col1GFP mice 3 days after injury

(a,b) Col1a2Cre:R26R^{tdTomato}:Col1GFP mice were subjected to ischemic cardiac injury and hearts harvested at 3 days post injury and stained for VECAD **(a)** tdTomato labeled cells (red, arrowheads) expressing VECAD (blue, arrowheads) but not GFP (green), with merged image demonstrating co-localization of tdTomato and VECAD but not GFP (arrowheads). Scale bar: 10 μm. **(b)** High magnification of a blood vessel (asterisk) outlined by VECAD staining (blue) demonstrating rare cell that colocalizes all three fluorophores (tdTomato +VECAD+GFP+, white, arrowhead). Arrows point to tdTomato positive cells expressing VECAD but not GFP. Scale bar: 10 μm. **(c–f)** Immunostaining for Cre protein on hearts of Col1a2Cre:R26R^{tdTomato}:Col1GFP harvested 3 days following ischemic injury to detect Cre expression in the nucleus of tdTomato labeled cells expressing VECAD. **(c)** TdTomato labeled cells in area of injury (arrowheads) expressing **(d)** VECAD (arrowheads) **(e)** merged image showing co-localization of fluorophores (arrowheads) **(f)** nuclei stained for DAPI and Cre demonstrating absence of any detectable nuclear Cre protein. Scale bar: 10μm **(g–i)** positive control demonstrating section of heart of Wt-1Cre transgenic mouse heart 3 days after injury with region of injury stained for **(g)** DAPI **(h)** Cre (red) and **(i)** merged image

demonstrating numerous cells in the injury region expressing nuclear Cre (arrowheads). Scale bar: 10μm **(j–m)** Cre immunostaining in tdTomato labeled cells expressing GFP. Area in region of injury with **(j)** nuclei stained for DAPI, **(k)** tdTomato expression (arrowhead) **(l)** GFP expression (arrowhead) and **(m)** merged image (DAPI, Cre and GFP) showing Cre staining (red channel) localized to the cytoplasm of GFP expressing cell (arrowhead). Scale bar: 10μm.

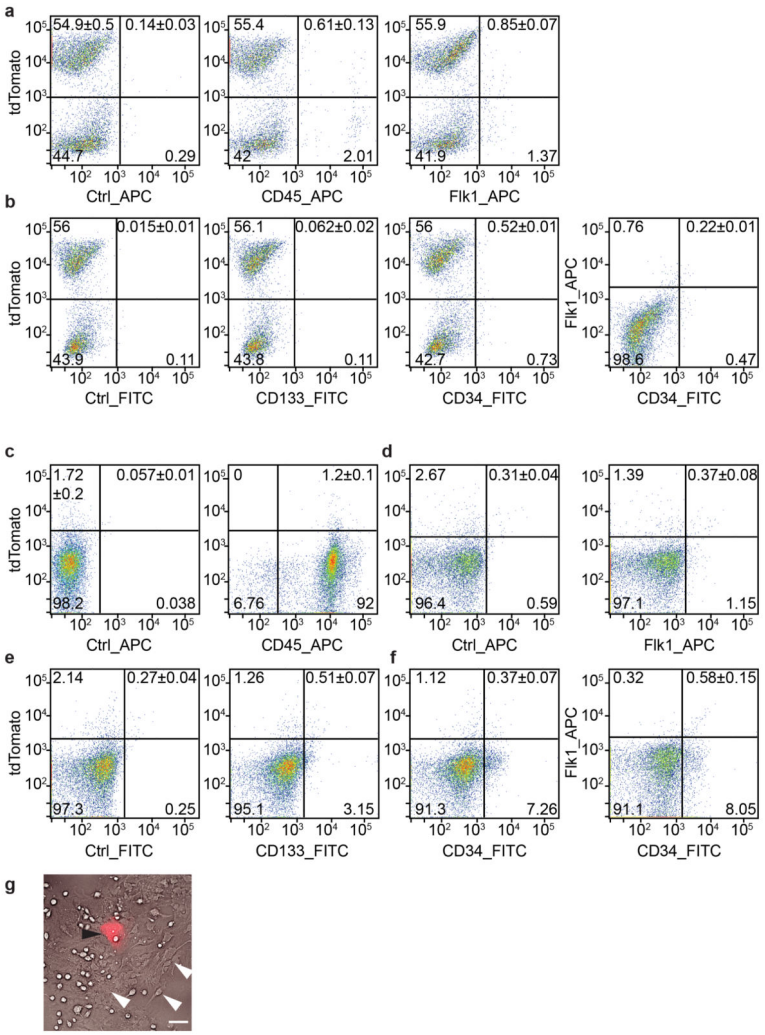

Extended Figure 5. Flow cytometry for endothelial progenitor markers on non-myocyte cells harvested from uninjured hearts of Col1a2CreERT:R26R^{tdTomato} mice and bone marrow cells isolated from the same animal

(a,b) Hearts of mice were digested, myocytes discarded and the entire non-myocyte population without any further selection was subjected to flow cytometry. Expression of tdTomato and **(a)** CD45 and Flk-1 (APC fluorophore) and **(b)** CD133, CD34 and combined expression of CD34 and Flk-1 in non-myocyte population. **(c–f)** Bone marrow cells were isolated from Col1a2CreERT:R26R^{tdTomato} mice and without further culture subjected to flow cytometry. Expression of tdTomato and (**c**) CD45 (**d**) Flk-1 (**e**) CD133 (**f**) CD34 and combined expression of Flk1 and CD34 in bone marrow cells (**g**) Expression of tdTomato in

bone marrow derived mesenchymal stem cell colonies (black arrowhead points to rare tdTomato positive cell, white arrowheads point to mesenchymal stem cells). Scale bar: 50μm.

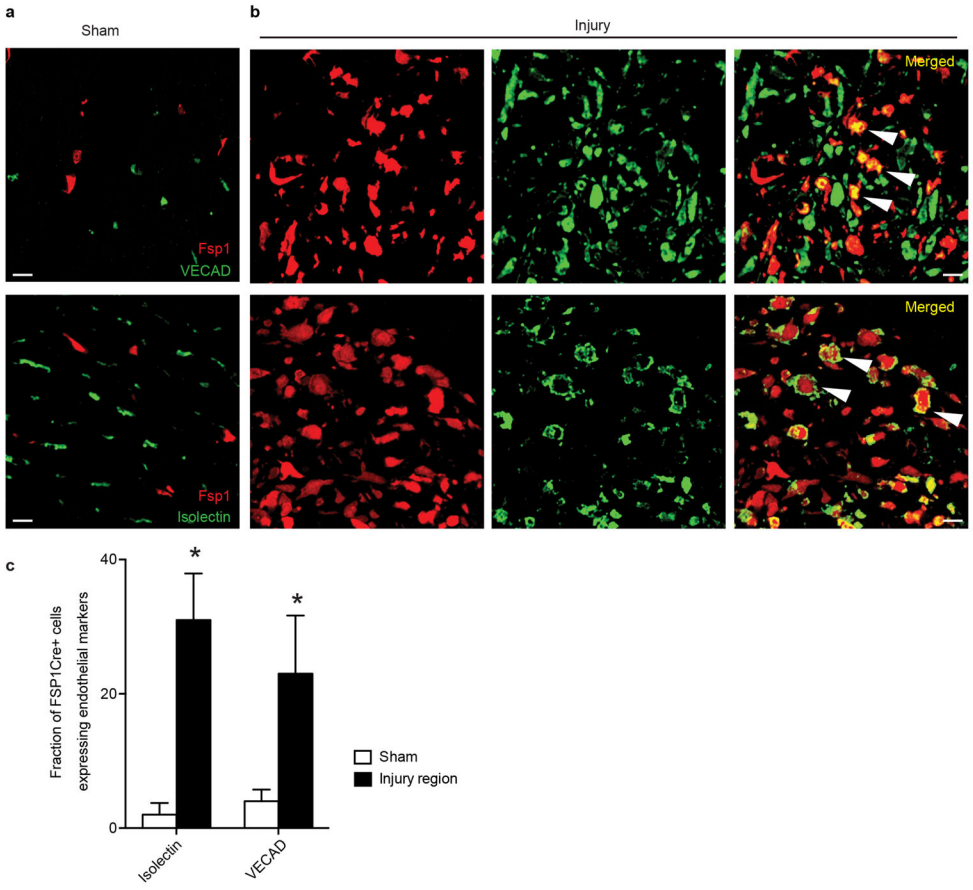

Extended Figure 6. MEndoT in FSP1Cre:R26R^{tdTomato} mice

FSP1Cre:R26R^{tdTomato} mice were subjected to (**a**) sham or (**b**) ischemia-reperfusion cardiac injury. Hearts were harvested 3 days after injury and stained for endothelial marker VECAD or isolectin. Injury region demonstrated tdTomato labeled cells expressing VECAD or isolectin (arrowheads, n=4). Scale bar: 10μm. (**c**) Quantitation of labeled fibroblasts that express VECAD or isolectin in sham injured animals and in the injury border zone (mean ±S.E.M., *p<0.01, n=4)

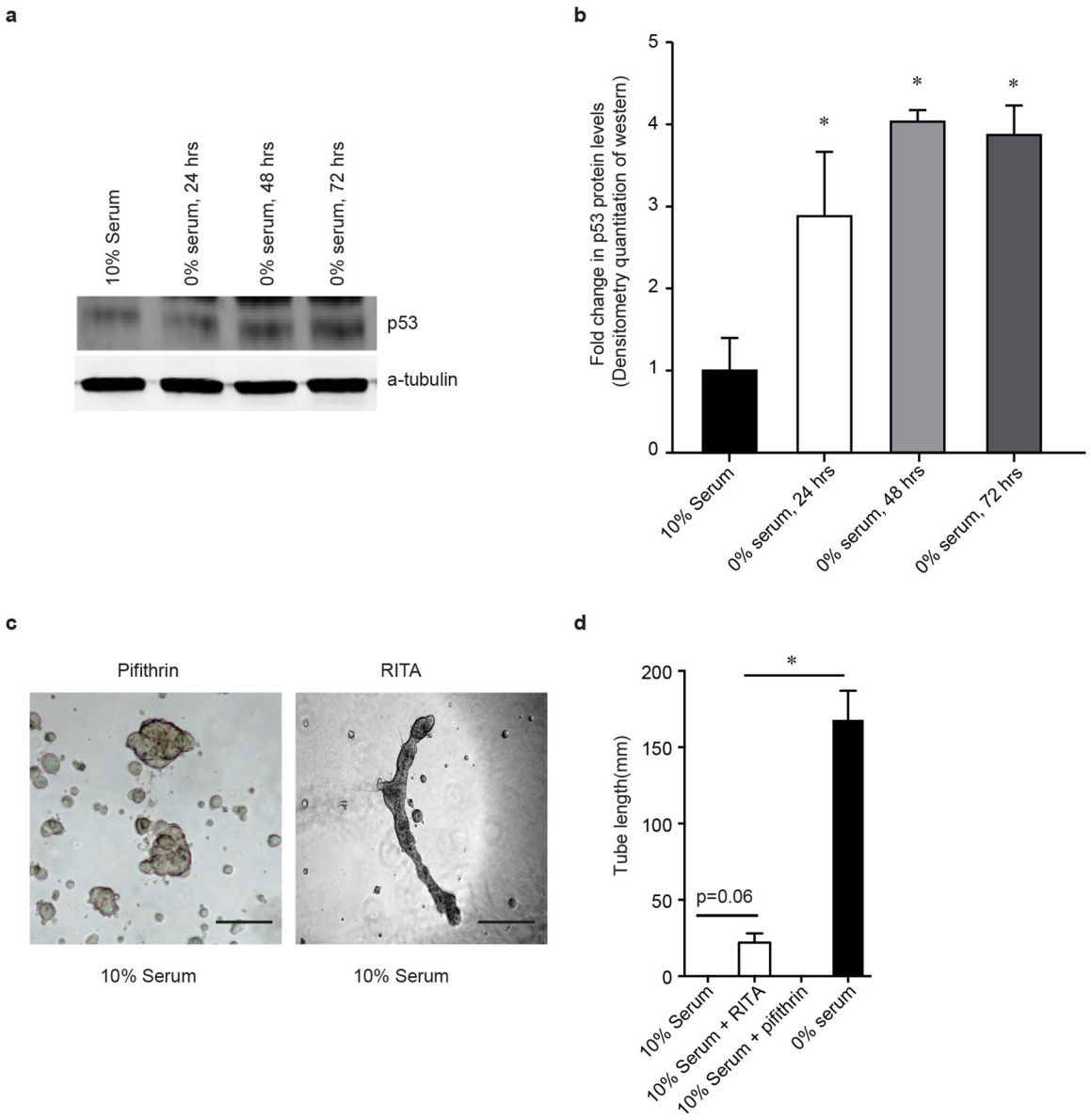

Extended Figure 7. Effect of serum starvation on p53 levels and effects of Pifithrin-α and RITA on tube formation of serum fed cardiac fibroblasts

(a) Western blot for p53 in cardiac fibroblasts subjected to serum starvation for 24, 48 and 72 hours (representative sample from n=3) **(b)** densitometric quantitation of Western blot (mean±S.E.M., *p<0.05 compared to cells in 10% serum). **(c)** Effect on tube formation after adding Pifithrin-α or RITA to cardiac fibroblasts grown in 10% serum Scale bar: 250μm **(d)** quantitation of tube formation (mean±S.E.M., *p<0.05, n=3)

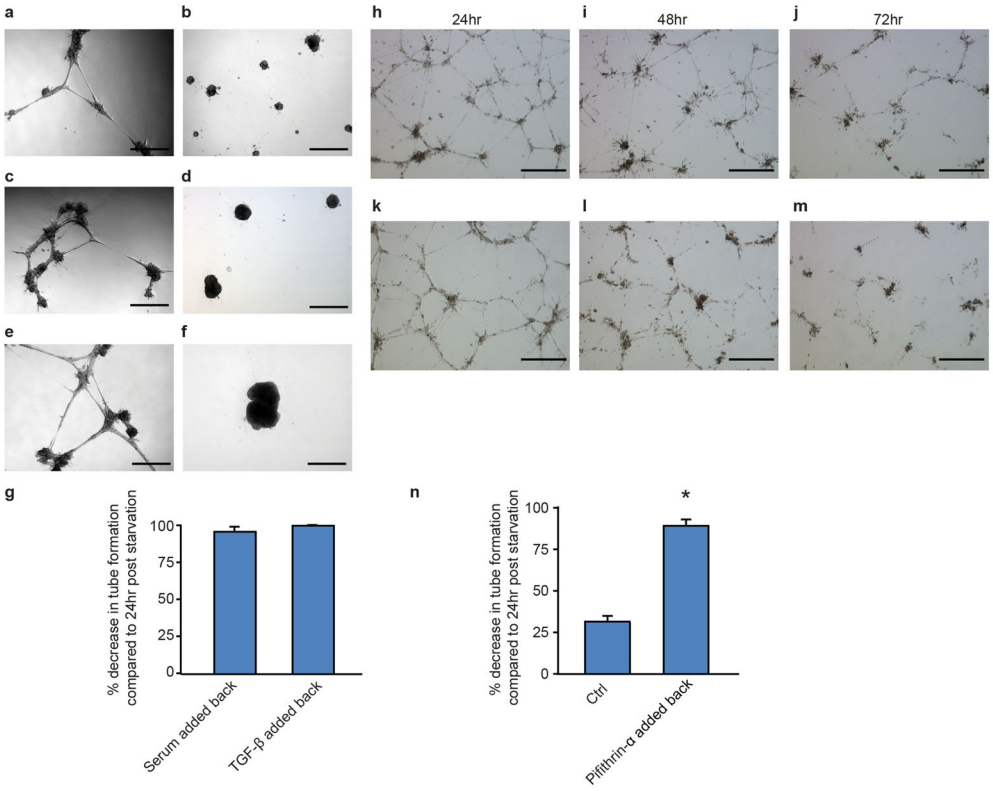

Extended Figure 8. Effect of adding TGFβ to serum starved cardiac fibroblasts, or adding TGFβ, serum or Pifithrin-α on tubes that have already formed

(a,b) Tube formation of cardiac fibroblasts subjected to serum starvation in the (**a**) absence or (**b**) presence of TGFβ. (TGFβ was added at the onset of serum starvation) Scale bar 50μm. (**c**–**f**) Effect of adding TGFβ or serum to tubes that had already formed. (**c,e**) twenty four hours following serum starvation (after tubes had already formed), PBS was added to tubes shown in c and e and photographs taken after another 24 hours. (**d,f**) After tubes had already formed (24 hours of serum starvation), (**d**) TGFβ or (**f**) serum was added and photographs taken after another 24 hours (note clumping of cells and regression of tubes in d and f). Scale bar: c–f: 50μm **(g)** Effect of adding TGFβ or serum to tubes that had already formed, expressed as a percentage decrease in tube length. (**h**–**n**) Effect of adding Pifithrin-α to serum starved cardiac fibroblasts that had already formed tubes. (**h,k**) Tube formation in cardiac fibroblasts serum starved for 24 hours in the absence of PBS or Pifithrin- α. Scale bar: 50μm **(i,j)** PBS was then added to cardiac fibroblasts shown in (h) and photographs were taken after another **(i)** 24 hours or **(j)** 48 hours of serum starvation. Scale bar: 50μm (**l, m**) Pifithrin-α was added to cardiac fibroblasts shown in (**k**) and photographs were taken after another (**l**) 24 hours or **(m)** 48 hours of serum starvation in the presence of Pifithrin-α. Scale bar: 50μm **(n)** Tube length in **(j)** and **(m)** was expressed as a percent change from their respective control **(h and k)** (mean±S.E.M. *$p<0.05$ compared to control, n=3).

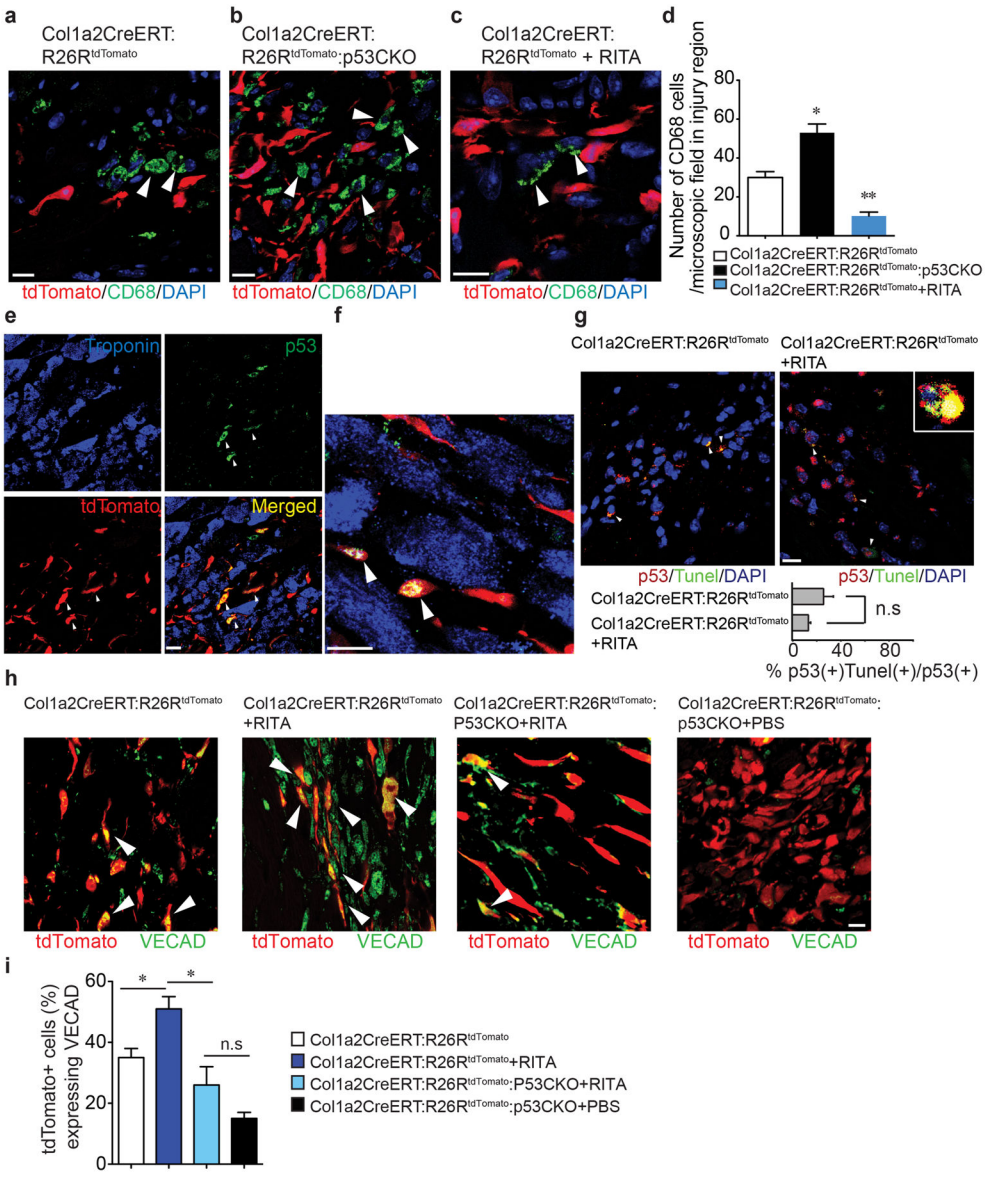

Extended Figure 9. RITA decreases inflammatory infiltrate after cardiac injury, does not increase apoptosis in myocytes and does not enhance MEndoT in Col1a2CreERT:R26R^{tdTomato}:p53CKO mice

(a–d) Sections of hearts harvested at 3 days following cardiac injury were stained for the monocyte/macrophage marker CD68 (green, arrowheads) in **(a)** Col1a2CreERT:R26R^{tdTomato}, **(b)** Col1a2CreERT:R26R^{tdTomato}:p53CKO and **(c)** RITA injected Col1a2CreERT:R26R^{tdTomato} Scale bar: 10μm. **(d)** quantification of the number of CD68 cells/high power field in the injury region (mean±S.E.M. *p<0.05 versus Col1a2CreERT:R26R^{tdTomato}, ** p<0.05 versus Col1a2CreERT:R26R^{tdTomato}, n=3) **(e–g)** p53 expression in myocytes after cardiac injury and effect of RITA on apoptosis in injury region. **(e,f)** Col1a2CreERT:R26R^{tdTomato} mice were subjected to ischemic cardiac injury, hearts harvested at 3 days and sections stained for p53 and cardiomyocyte marker Troponin. **(e)** p53 (green, arrowheads) staining is observed in tdTomato expressing cells (red,

arrowheads) but not in cardiomyocytes (blue), merged image shows arrowheads pointing to tdTomato labeled cells expressing p53. Scale bar: 10μm. (**f**) Higher magnification in injury region demonstrating tdTomato cells (arrowheads) expressing p53 (merged, yellow, arrowheads) but p53 staining is not visible in cardiomyocytes (blue). Scale bar: 10μm. (**g**) TUNEL staining and quantification to determine p53+ apoptotic cells after RITA injection (arrowheads point to p53+TUNEL+ cells in Col1a2CreERT:R26R^{tdTomato} mice (left panel) and RITA injected Col1a2CreERT:R26R^{tdTomato} mice (right panel), inset shows p53+TUNEL+ cell in higher magnification (data shown as mean±S.E.M, ns=not significant, n=3). Hearts in both cases were examined 3 days after injury. Scale bar: 10μm. **(h,i)** Effect of RITA on MEndoT in Col1a2CreERT:R26R^{tdTomato}:p53CKO mice after cardiac injury. **(h)** tdTomato labeled cardiac fibroblasts expressing VECAD in Col1a2CreERT:R26R^{tdTomato} mice treated with/without RITA, Col1a2CreERT:R26R^{tdTomato}:p53CKO mice treated with/without RITA. Scale bar: 10μm. **(i)** Quantitation of the percentage of labeled fibroblasts undergoing MEndoT for each treatment group (mean ±S.E.M., *$p<0.05$, n.s= not significant, n=4 animals/group).

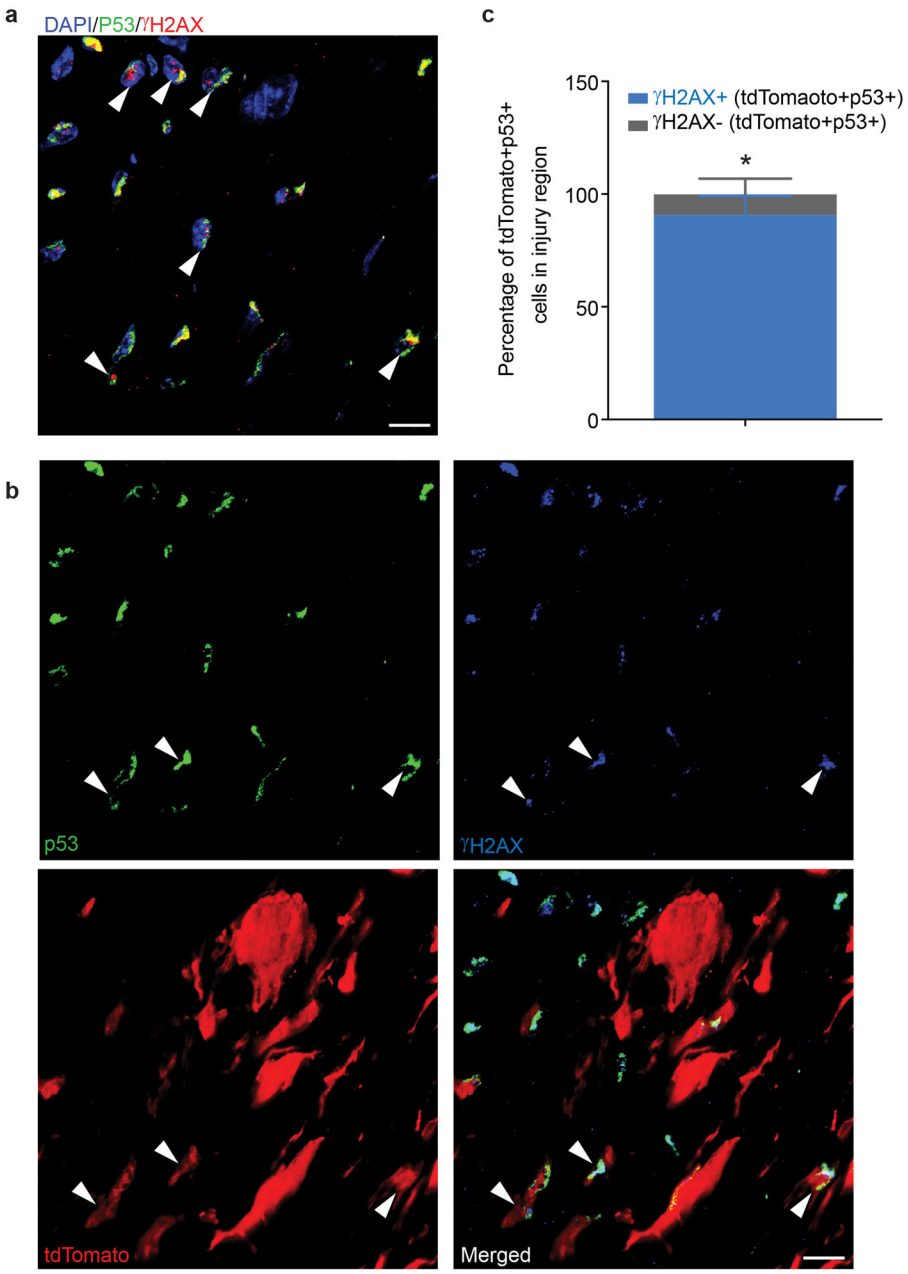

Extended Figure 10. γH2AX expression in cells expressing p53 after ischemic cardiac injury

Col1a2CreERT:R26R^{tdTomato} mice were subjected to ischemic cardiac injury and immunostaining performed for γH2AX and p53. (**a**) Immunostaining for p53 (green), γH2AX (red) and DAPI (blue) in region of injury (arrowheads point to nuclei co-expressing γH2AX and p53). Scale bar: 10μm. (**b**) Immunostaining for p53 (green), γH2AX (blue) and tdTomato (red) to determine co-expression of p53 and γH2AX in tdTomato labeled cells. Arrowheads point to tdTomato positive cells co-expressing γH2AX and p53. Scale bar: 10μm. (**c**) quantitation of the fraction of tdTomato+p53+ cells expressing γH2AX (mean ±S.E.M. *p<0.01, n=3).

Supplementary Material

Refer to Web version on PubMed Central for supplementary material.

Acknowledgments

We thank the Michael Hooker Confocal Microscopy and the Histology Research Core facilities at UNC, Chapel Hill. We thank the confocal and advanced light microscopy facilities in the Division of Molecular Medicine and California Nanosystems Institute at UCLA, Histology facilities at Brain Research Institute & Pathology and Laboratory Medicine, UCLA, Broad Stem Cell Research Center UCLA flow cytometry laboratories and the Vector core facility at UCLA for technical assistance. We thank Kathleen Caron, Vicki Bauch, Joan Taylor, Carol Otey at UNC, Chapel Hill and Jake Lusis at UCLA for scientific suggestions and discussion. This work was supported by grants from the National Institutes of Health (NIH R01HL102190) to Arjun Deb. Super-resolution studies and ChIP studies were supported by NIH grant HL088640 to ES and NIH grant HL105699 to TV. Eric Ubil was supported in part by a pre-doctoral grant from the American Heart Association.

References

1. Christia P, et al. Systematic characterization of myocardial inflammation, repair, and remodeling in a mouse model of reperfused myocardial infarction. J Histochem Cytochem. 2013; 61:555–570. [PubMed: 23714783]
2. Cohn JN, Ferrari R, Sharpe N. Cardiac remodeling--concepts and clinical implications: a consensus paper from an international forum on cardiac remodeling. Behalf of an International Forum on Cardiac Remodeling. J Am Coll Cardiol. 2000; 35:569–582. [PubMed: 10716457]
3. Kocher AA, et al. Neovascularization of ischemic myocardium by human bone-marrow-derived angioblasts prevents cardiomyocyte apoptosis, reduces remodeling and improves cardiac function. Nat Med. 2001; 7:430–436. [PubMed: 11283669]
4. Souders CA, Bowers SL, Baudino TA. Cardiac fibroblast: the renaissance cell. Circ Res. 2009; 105:1164–1176. [PubMed: 19959782]
5. Zeisberg EM, et al. Endothelial-to-mesenchymal transition contributes to cardiac fibrosis. Nat Med. 2007; 13:952–961. [PubMed: 17660828]
6. Chintalgattu V, Nair DM, Katwa LC. Cardiac myofibroblasts: a novel source of vascular endothelial growth factor (VEGF) and its receptors Flt-1 and KDR. J Mol Cell Cardiol. 2003; 35:277–286. [PubMed: 12676542]
7. Zhao L, Eghbali-Webb M. Release of pro- and anti-angiogenic factors by human cardiac fibroblasts: effects on DNA synthesis and protection under hypoxia in human endothelial cells. Biochim Biophys Acta. 2001; 1538:273–282. [PubMed: 11336798]
8. Qian L, et al. In vivo reprogramming of murine cardiac fibroblasts into induced cardiomyocytes. Nature. 2012; 485:593–598. [PubMed: 22522929]
9. Song K, et al. Heart repair by reprogramming non-myocytes with cardiac transcription factors. Nature. 2012; 485:599–604. [PubMed: 22660318]
10. Duan J, et al. Wnt1/betacatenin injury response activates the epicardium and cardiac fibroblasts to promote cardiac repair. EMBO J. 2012; 31:429–442. [PubMed: 22085926]
11. Zheng B, Zhang Z, Black CM, de Crombrugghe B, Denton C. Ligand-dependent genetic recombination in fibroblasts : a potentially powerful technique for investigating gene function in fibrosis. Am J Pathol. 2002; 160:1609–1617. [PubMed: 12000713]
12. Liu S, Thompson K, Leask A. CCN2 expression by fibroblasts is not required for cutaneous tissue repair. Wound repair and regeneration. 2014; 22:119–124. [PubMed: 24393160]
13. Madisen L, et al. A robust and high-throughput Cre reporting and characterization system for the whole mouse brain. Nat Neurosci. 2010; 13:133–140. [PubMed: 20023653]
14. Dejana E. Endothelial cell-cell junctions: happy together. Nat Rev Mol Cell Biol. 2004; 5:261–270. [PubMed: 15071551]
15. Singh H, et al. Visualization and quantification of cardiac mitochondrial protein clusters with STED microscopy. Mitochondrion. 2012; 12:230–236. [PubMed: 21982778]

16. Li Y, et al. Direct labeling and visualization of blood vessels with lipophilic carbocyanine dye DiI. Nat Protoc. 2008; 3:1703–1708. [PubMed: 18846097]
17. Urbich C, Dimmeler S. Endothelial progenitor cells: characterization and role in vascular biology. Circ Res. 2004; 95:343–353. [PubMed: 15321944]
18. Tomasek JJ, Gabbiani G, Hinz B, Chaponnier C, Brown RA. Myofibroblasts and mechano-regulation of connective tissue remodelling. Nat Rev Mol Cell Biol. 2002; 3:349–363. [PubMed: 11988769]
19. Weber KT, Sun Y, Bhattacharya SK, Ahokas RA, Gerling IC. Myofibroblast-mediated mechanisms of pathological remodelling of the heart. Nat Rev Cardiol. 2013; 10:15–26. [PubMed: 23207731]
20. Zhou B, et al. Adult mouse epicardium modulates myocardial injury by secreting paracrine factors. J Clin Invest. 2011; 121:1894–1904. [PubMed: 21505261]
21. Acharya A, et al. The bHLH transcription factor Tcf21 is required for lineage-specific EMT of cardiac fibroblast progenitors. Development. 2012; 139:2139–2149. [PubMed: 22573622]
22. Lin SL, Kisseleva T, Brenner DA, Duffield JS. Pericytes and perivascular fibroblasts are the primary source of collagen-producing cells in obstructive fibrosis of the kidney. Am J Pathol. 2008; 173:1617–1627. [PubMed: 19008372]
23. Melo LG, et al. Molecular and cell-based therapies for protection, rescue, and repair of ischemic myocardium: reasons for cautious optimism. Circulation. 2004; 109:2386–2393. [PubMed: 15159329]
24. Sharpless NE, DePinho RA. p53: good cop/bad cop. Cell. 2002; 110:9–12. [PubMed: 12150992]
25. Hong H, et al. Suppression of induced pluripotent stem cell generation by the p53-p21 pathway. Nature. 2009; 460:1132–1135. [PubMed: 19668191]
26. Chang CJ, et al. p53 regulates epithelial-mesenchymal transition and stem cell properties through modulating miRNAs. Nat Cell Biol. 2011; 13:317–323. [PubMed: 21336307]
27. Hasan NM, Adams GE, Joiner MC. Effect of serum starvation on expression and phosphorylation of PKC-alpha and p53 in V79 cells: implications for cell death. Int J Cancer. 1999; 80:400–405. [PubMed: 9935181]
28. Shi Y, et al. Starvation-induced activation of ATM/Chk2/p53 signaling sensitizes cancer cells to cisplatin. BMC cancer. 2012; 12:571. [PubMed: 23211021]
29. Komarov PG, et al. A chemical inhibitor of p53 that protects mice from the side effects of cancer therapy. Science. 1999; 285:1733–1737. [PubMed: 10481009]
30. Marino S, Vooijs M, van Der Gulden H, Jonkers J, Berns A. Induction of medulloblastomas in p53-null mutant mice by somatic inactivation of Rb in the external granular layer cells of the cerebellum. Genes Dev. 2000; 14:994–1004. [PubMed: 10783170]
31. Issaeva N, et al. Small molecule RITA binds to p53, blocks p53-HDM-2 interaction and activates p53 function in tumors. Nat Med. 2004; 10:1321–1328. [PubMed: 15558054]
32. Bruhl T, et al. Homeobox A9 transcriptionally regulates the EphB4 receptor to modulate endothelial cell migration and tube formation. Circ Res. 2004; 94:743–751. [PubMed: 14764452]
33. Boudreau N, Andrews C, Srebrow A, Ravanpay A, Cheresh DA. Induction of the angiogenic phenotype by Hox D3. J Cell Biol. 1997; 139:257–264. [PubMed: 9314544]
34. Fazel S, et al. Cardioprotective c-kit+ cells are from the bone marrow and regulate the myocardial balance of angiogenic cytokines. J Clin Invest. 2006; 116:1865–1877. [PubMed: 16823487]
35. Economopoulou M, et al. Histone H2AX is integral to hypoxia-driven neovascularization. Nat Med. 2009; 15:553–558. [PubMed: 19377486]
36. Webster KA, et al. Hypoxia-activated apoptosis of cardiac myocytes requires reoxygenation or a pH shift and is independent of p53. J Clin Invest. 1999; 104:239–252. [PubMed: 10430605]
37. Bolte S, Cordelieres FP. A guided tour into subcellular colocalization analysis in light microscopy. J Microsc. 2006; 224:213–232. [PubMed: 17210054]
38. McDonald JH, Dunn KW. Statistical tests for measures of colocalization in biological microscopy. J Microsc. 2013; 252:295–302. [PubMed: 24117417]
39. Agocha AE, Eghbali-Webb M. A simple method for preparation of cultured cardiac fibroblasts from adult human ventricular tissue. Mol Cell Biochem. 1997; 172:195–198. [PubMed: 9278245]

40. Nagelkerke JF, Barto KP, van Berkel TJ. In vivo and in vitro uptake and degradation of acetylated low density lipoprotein by rat liver endothelial, Kupffer, and parenchymal cells. J Biol Chem. 1983; 258:12221–12227. [PubMed: 6313644]

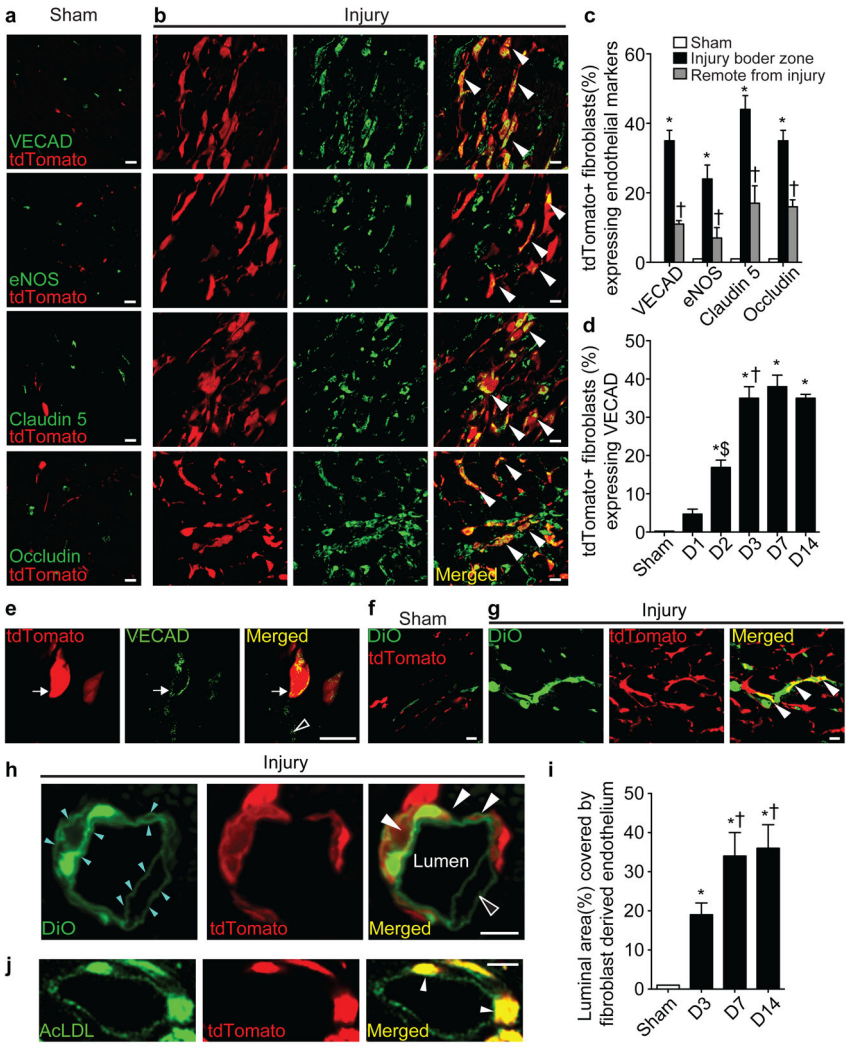

Figure 1. Cardiac fibroblasts adopt endothelial cell fates after cardiac injury

(a,b) Hearts from Col1a2CreERT:R26R^{tdTomato} immunostained for endothelial markers (arrowheads) (**c**) tdTomato+ fibroblasts(%) expressing endothelial markers (*p<0.05 vs sham, † p<0.05 vs injury border zone). (**d**) Temporal expression of VECAD (* p<0.005 vs sham, †p<0.05 vs Day 1 and 2, $ p<0.05 vs Day 1,). (**e**) STED microscopy demonstrating tdTomato+VECAD+ cell (arrowhead; unfilled arrowhead shows tdTomato- endothelial cell) (**f–h**) DiO stained capillary in (**f,g**) longitudinal section (arrowheads show tdTomato+DiO+ cells) or (**h**) cross-section (cyan arrowheads show DiO stained inner and outer endothelial cell membranes, white arrowheads show tdTomato+ endothelial cell; unfilled arrowhead shows tdTomato- endothelial cell). Scale bar: 5μm. (**i**) Luminal surface area occupied by fibroblast derived endothelium (* p<0.005 vs sham, † p<0.05 vs Day 3). (**j**) AcLDL uptake by tdTomato+ endothelium (arrowheads). (n=3 animals /group/ time point, All graphs show mean±S.E.M., scale bar:10μm unless mentioned)

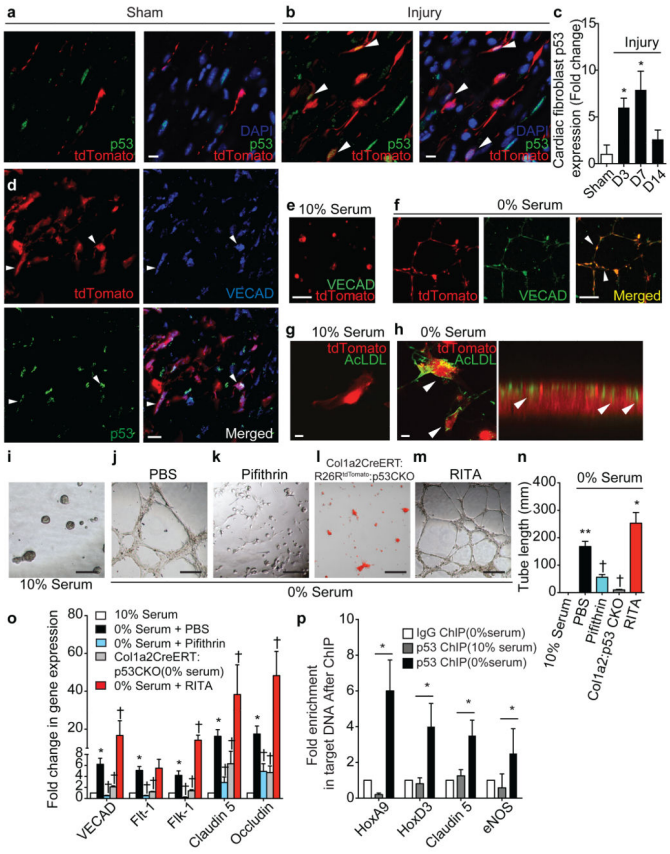

Figure 2. Cardiac fibroblasts upregulate p53 after injury and p53 mediates MEndoT *ex vivo*

(a,b) p53 immunostaining in injured hearts (arrowheads show tdTomato+P53+ cells) **(c)** Temporal p53 expression in labeled fibroblasts (*p<0.05 vs sham, n=3 animals/time point). **(d)** co-expression of p53, VECAD & tdTomato (arrowhead). **(e,f)** tdTomato+VECAD+ tubes and **(g,h)** AcLDL uptake after serum starvation (arrowheads, n=4). Scale bar: 250μm **(h, right panel)** Confocal image (XZ plane) showing AcLDL internalization (Scale bar: 20μm) **(i–m)** Tube formation of cardiac fibroblasts in **(i)**10% serum or 0% serum with **(j)** PBS **(k)** 100μM Pifithrin-α, **(m)** 0.1μM RITA, or **(l)** p53 deletion (bright field and fluorescence overlay). Scale bar: 250μm **(n)** Quantitation of tube length (** p<0.005 vs 10% serum. † p<0.005 and *p<0.05 vs starved cells, n=3). **(o)** Endothelial gene expression in cardiac fibroblasts (* p<0.005 vs 10% serum, † p<0.05 vs PBS, n=8). **(p)** ChIP with p53 (*p<0.05). (All graphs show mean±S.E.M., scale bar: 10μm unless mentioned).

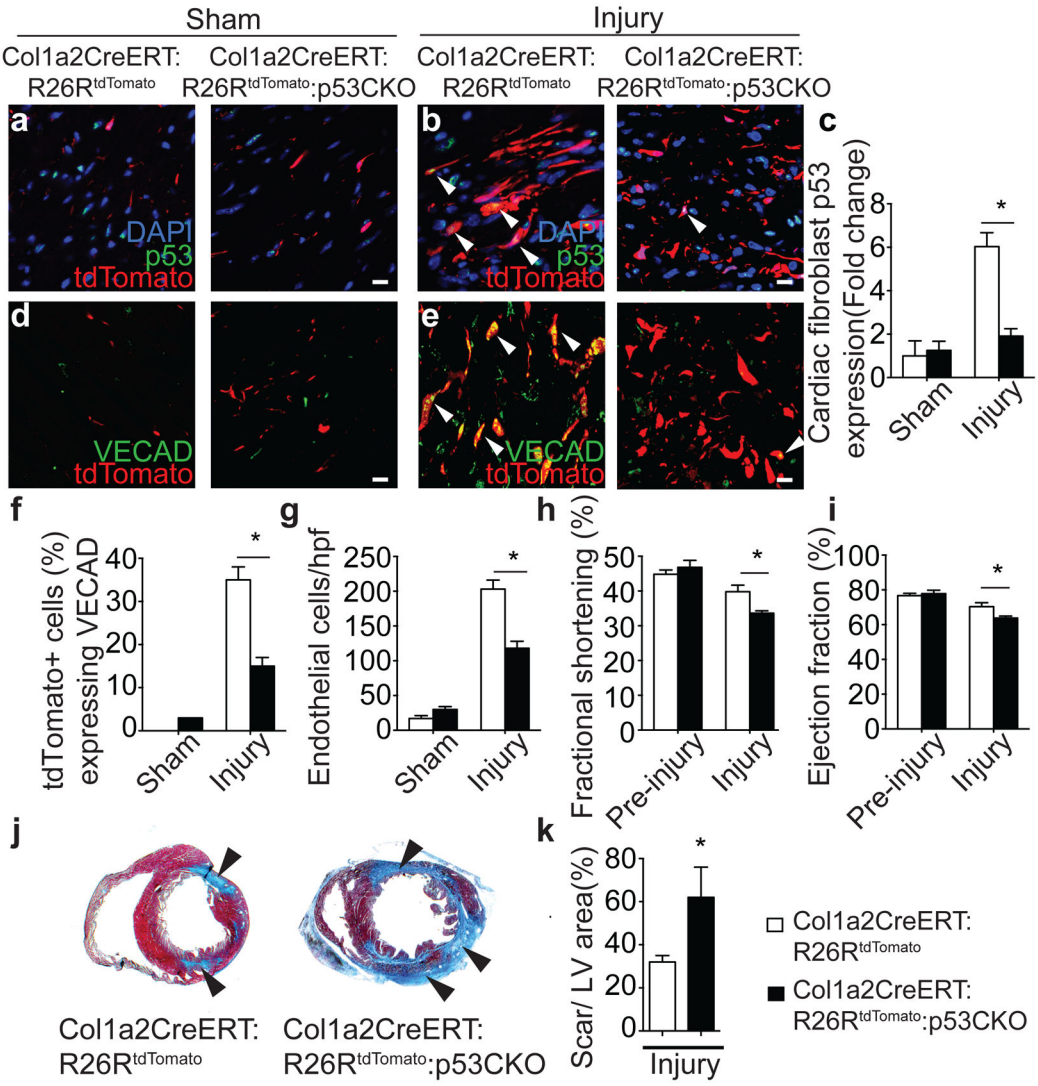

Figure 3. MEndoT after cardiac injury is p53 dependent

(a–c) p53 immunostaining in Col1a2CreERT:R26R^{tdTomato} and Col1a2CreERT:R26R^{tdTomato}:p53CKO hearts (arrowheads) and (**c**) quantification of p53 expression in labeled fibroblasts (* p<0.005). (**d–f**) VECAD immunostaining in labeled fibroblasts (arrowheads) and (**f**) Labeled fibroblasts(%) expressing VECAD (* p<0.005). (**g**) Number of endothelial cells/high power field (* p<0.005, n=5 animals) (**h,i**) Cardiac function prior to and 7 days after injury. (*p<0.05, n=9 animals). (**j**) Masson's Trichrome staining 14 days after injury. (**k**) Quantitation of fibrosis (* p<0.05). (n=4 animals unless mentioned, All graphs show mean±S.E.M., scale bar: 10μm).

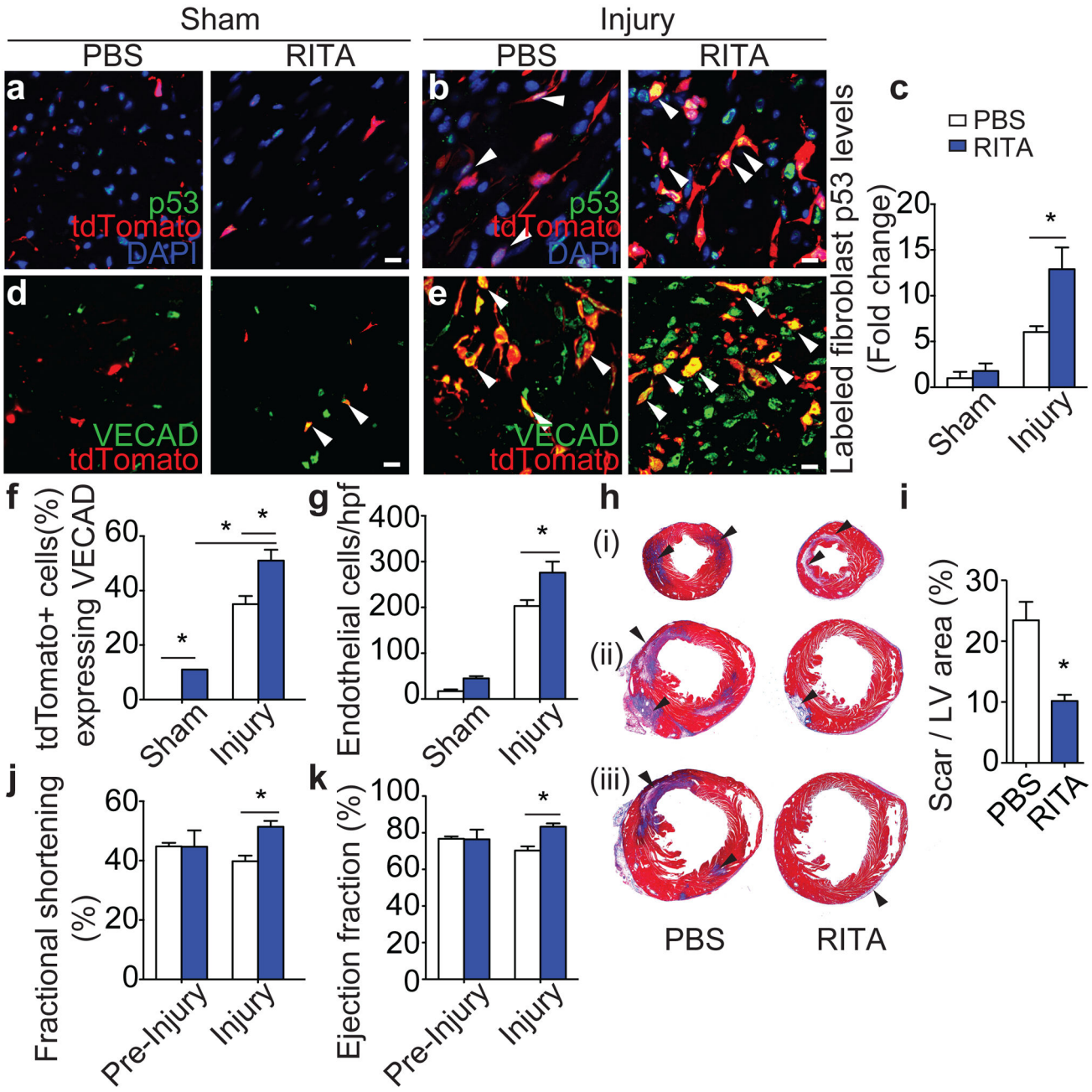

Figure 4. RITA enhances MEndoT after cardiac injury

Hearts from PBS or RITA treated Col1a2CreERT:R26R^{tdTomato} mice (**a,b**) p53 immunostaining in labeled fibroblasts (arrowheads) and (**c**) quantitation of p53 expression (* p<0.005). (**d–e**) VECAD immunostaining in labeled fibroblasts (arrowheads). (**f**) Labeled fibroblasts(%) expressing VECAD (* p<0.05). (**g**) Endothelial cells/hpf (* p<0.05). (**h**) Masson's Trichrome staining (blue, arrowheads) near (**i**) apex, (ii) between mid-ventricle and apex and (iii) mid-ventricle (n=14 animals) (i) Quantitation of fibrosis (* p<0.001, n=14

animals). (**j,k**) Cardiac function prior to and 7 days after injury. (* $p<0.05$, n=8 animals). (n=4 animals unless mentioned, All graphs show mean ± S.E.M., scale bar: 10μm).